Electronic Research Archive

http://www.aimspress.com/journal/era

ERA, 31(9): 5124–5150.
DOI: 10.3934/era.2023262
Received: 06 May 2023
Revised: 15 June 2023
Accepted: 28 June 2023
Published: 17 July 2023

Research article

Bifurcations, stability switches and chaos in a diffusive predator-prey model with fear response delay

Mengting Sui and Yanfei Du*

School of Mathematics and Data Science, Shaanxi University of Science and Technology, Xi'an 710021, China

* **Correspondence:** Email: duyanfei@sust.edu.cn.

Abstract: Recent studies demonstrate that the reproduction of prey is suppressed by the fear of predators. However, it will not respond immediately to fear, but rather reduce after a time lag. We propose a diffusive predator-prey model incorporating fear response delay into prey reproduction. Detailed bifurcation analysis reveals that there are three different cases for the effect of the fear response delay on the system: it might have no effect, both stabilizing and destabilizing effect, or destabilizing effect on the stability of the positive equilibrium, respectively, which are found by numerical simulations to correspond to low, intermediate or high level of fear. For the second case, through ordering the critical values of Hopf bifurcation, we prove the existence of stability switches for the system. Double Hopf bifurcation analysis is carried out to better understand how the fear level and delay jointly affect the system dynamics. Using the normal form method and center manifold theory, we derive the normal form of double Hopf bifurcation, and obtain bifurcation sets around double Hopf bifurcation points, from which all the dynamical behaviors can be explored, including periodic solutions, quasi-periodic solutions and even chaotic phenomenon.

Keywords: predator-prey system; fear response delay; stability switches; double Hopf bifurcation; normal form

1. Introduction

The interaction between predator and prey is one of the most important topics in mathematical biology and theoretical ecology [1]. The direct interaction, which is reflected by predation, has been extensively studied [2–5]. Recently, a field experimental study [6] provided evidence that show that indirect effect (e.g., fear effect) cannot be ignored. Even though there is no direct killing between predators and prey, the presence of predators cause a reduction in prey population [6, 7] . To explore the impact that fear can have on population dynamics, Wang et al. [8] formulated the following model

incorporating the cost of fear

$$\begin{cases} \frac{\mathrm{d}u}{\mathrm{d}t} = f(k, v(t))r_0u(t) - du(t) - au^2(t) - g(u(t))v(t), \\ \\ \frac{\mathrm{d}v}{\mathrm{d}t} = cg(u(t))v(t) - mv(t), \end{cases} \tag{1.1}$$

where u and v are the population densities of the prey and predator, respectively. Function $f(k, v(t))$ reflects the cost of anti-predation response due to fear, where k measures the level of fear. r_0 is the reproduction rate of prey in the absence of predator, d and m represent the natural death rate, a reflects the death rate due to intra-specific competition, the positive constant c is the efficiency in biomass transfer, $g(u(t))$ is the functional response. After their work, other biological phenomena, such as the Allee effect, harvesting, cooperation hunting, prey refuge, group defense and so on, were introduced into predator-prey models with the fear effect [1, 9–15].

In fact, besides the cost in the reproduction of prey due to fear, there are also some benefits for an anti-predation response. Wang and Zou [16] described such benefits with $g(u(t), k)$ instead of $g(u(t))$, and considered both linear functional response and Holling type II functional response. In the model with the Holling type II functional response, they choose $g(u(t), k) = \frac{1}{1+c_1k} \cdot \frac{pu(t)}{1+qu(t)}$, $f(k, v) = \frac{1}{1+c_2kv(t)}$ and get the following model

$$\begin{cases} \frac{\mathrm{d}u}{\mathrm{d}t} = \frac{r_0u(t)}{1+c_2kv(t)} - du(t) - au^2(t) - \frac{pu(t)v(t)}{1+qu(t)} \cdot \frac{1}{1+c_1k}, \\ \\ \frac{\mathrm{d}v}{\mathrm{d}t} = \frac{pu(t)v(t)}{1+qu(t)} \cdot \frac{c}{1+c_1k} - mv(t), \end{cases} \tag{1.2}$$

where c_1, c_2 represent the decreasing rate of reproduction and predation, respectively.

To obtain more resources, species tend to migrate from a high population density area to a low population density area. Therefore, spatial diffusion should be considered when we model the interaction between predator and prey. Many diffusive models have been proposed to investigate the influence of the cost of fear on the spatial distribution of species [17–20]. Wang and Zou [21] proposed a reaction-diffusion-advection predator prey model, in which conditions of spatial pattern formation are obtained.

In reality, there are time delays in almost every process of predator and prey interaction. Many kinds of delays have been incorporated into predator-prey models with the fear effect [16–18, 22–25]. Since the biomass transfer is not instantaneous after the predation of prey, the biomass transfer delay is considered in [16]. A generation time delay in prey has been considered in [23]. In fact, the reproduction of prey will not respond immediately to fear, but will rather reduce after a time lag. Such a fear response delay has been considered in [18, 24, 25].

Motivated by [16] and the previous work, we propose the following model

$$\begin{cases} \frac{\partial}{\partial t}u(x,t) = d_1\Delta u(x,t) + \frac{r_0u(x,t)}{1+c_2kv(x,t-\tau)} - du(x,t) - au^2(x,t) \\ \qquad\qquad - \frac{pu(x,t)v(x,t)}{1+qu(x,t)} \cdot \frac{1}{1+c_1k}, & x \in (0, l\pi),\ t > 0, \\ \\ \frac{\partial}{\partial t}v(x,t) = d_2\Delta v(x,t) + \frac{pu(x,t)v(x,t)}{1+qu(x,t)} \cdot \frac{c}{1+c_1k} - mv(x,t), & x \in (0, l\pi),\ t > 0, \\ \\ u_x(0,t) = u_x(l\pi,t) = v_x(0,t) = v_x(l\pi,t) = 0, & t > 0, \\ \\ u(x,t) = u_0(x,t) \geqslant 0, v(x,t) = v_0(x,t) \geqslant 0, & x \in (0, l\pi), t \in [-\tau, 0], \end{cases} \tag{1.3}$$

where $d_1, d_2 > 0$ represent the diffusion coefficients of prey and predator, respectively, and τ is the fear response delay in prey reproduction.

Although there have been some literature on a predator-prey model with fear effect and delay, no work has been done to explore the joint impact of fear level and fear response delay on the population dynamics. In this paper, we aim to reveal how these two parameters k and τ jointly affect the dynamics of system (1.3) from the view of bifurcation analysis. The characteristic equation may have no, one or two pairs of purely imaginary roots under different conditions. Correspondingly, the fear response delay may have no effect, both stabilizing and destabilizing effect, or destabilizing effect on the stability of the positive equilibrium. By the discussion of the monotonicity of the critical values of Hopf bifurcation, we get the order of all the Hopf bifurcation values. We prove the existence of stability switches for system (1.3) under suitable condition. Through numerical simulations, we find that the level of fear k has a crucial role in the stability of positive equilibrium and the occurrence of Hopf bifurcation induced by fear response delay. To reveal the complex phenomena induced by k and τ, double Hopf bifurcation analysis is carried out, which can induce complex spatio-temporal dynamics [26, 27]. It provides a qualitative classification of dynamical behaviors on the (k, τ) plane, which can help us to explicitly observe the different dynamics corresponding to different values of k and τ, including quasi-periodic oscillations on two or three dimensional torus, and even chaos.

The rest of this paper is organized as follows. In Section 2, we analyze the local stability of equilibria and obtain the condition of Hopf bifurcation in three different cases. In Section 3, we give the condition for double Hopf bifurcation and derive the normal form of the double Hopf bifurcation. In Section 4, numerical simulations are presented to verify our theoretical results. Finally, conclusions and discussions are given in Section 5.

2. Local stability and Hopf bifurcation

In this section, we discuss the local stability of equilibria. System (1.3) has three possible equilibria. The trivial equilibrium $E_0(0, 0)$ always exists. When $r_0 - d > 0$, system (1.3) has a predator-free equilibrium $E_u(\frac{r_0-d}{a}, 0)$. Moreover, if

$$\text{(H1)} \quad 0 < \frac{m(1 + c_1k)}{pc - mq(1 + c_1k)} < \frac{r_0 - d}{a}$$

holds, there is a unique positive equilibrium $E^*(u^*, v^*)$, where

$$u^* = \frac{m(1 + c_1k)}{pc - mq(1 + c_1k)}, \quad v^* = \frac{-a_1 + \sqrt{a_1^2 - 4a_0a_2}}{2a_0}, \tag{2.1}$$

with

$$\begin{cases} a_0 = c_2pk, \\ a_1 = p + (d + au^*)(1 + qu^*)(1 + c_1k)c_1k, \\ a_2 = (d + au^* - r_0)(1 + qu^*)(1 + c_1k). \end{cases} \tag{2.2}$$

It is well known that the laplacian operator Δ has eigenvalues $-n^2/l^2$ $(n = 0, 1, 2, \cdots)$.

Now, we study the local stability for each of equilibria. The linearization of system (1.3) at an equilibrium $(\bar{u}, \bar{v})$ can be written as

$$\frac{\partial}{\partial t}\begin{pmatrix} u(x,t) \\ v(x,t) \end{pmatrix} = D\begin{pmatrix} \Delta u(x,t) \\ \Delta v(x,t) \end{pmatrix} + G_0\begin{pmatrix} u(x,t) \\ v(x,t) \end{pmatrix} + G_1\begin{pmatrix} u(x,t-\tau) \\ v(x,t-\tau) \end{pmatrix}, \tag{2.3}$$

where

$$D = \begin{pmatrix} d_1 & 0 \\ 0 & d_2 \end{pmatrix}, \ G_0 = \begin{pmatrix} J_{11} & J_{12} \\ J_{21} & J_{22} \end{pmatrix}, \ G_1 = \begin{pmatrix} 0 & K_{12} \\ 0 & 0 \end{pmatrix},$$

with

$$\begin{aligned} &J_{11} = \tfrac{r_0}{1+c_2k\bar{v}} - d - 2a\bar{u} - \tfrac{p\bar{v}}{(1+c_1k)(1+q\bar{u})^2}, \quad J_{12} = -\tfrac{p\bar{u}}{(1+c_1k)(1+q\bar{u})}, \\ &J_{21} = \tfrac{cp\bar{v}}{(1+c_1k)(1+q\bar{u})^2,} \quad J_{22} = \tfrac{cp\bar{u}}{(1+q\bar{u})(1+c_1k)} - m, \quad K_{12} = -\tfrac{r_0c_2k\bar{u}}{(1+c_2k\bar{v})^2}. \end{aligned}$$

The characteristic equation is given by

$$\det\begin{pmatrix} \lambda + d_1\frac{n^2}{l^2} - J_{11} & -J_{12} - K_{12}e^{-\lambda\tau} \\ -J_{21} & \lambda + d_2\frac{n^2}{l^2} - J_{22} \end{pmatrix} = 0, \ \ n = 0, 1, 2, \cdots. \tag{2.4}$$

From (2.4), we get the corresponding characteristic equation at $E_0(0, 0)$ as

$$(\lambda + d_1\frac{n^2}{l^2} - r_0 + d)(\lambda + d_2\frac{n^2}{l^2} + m) = 0, \ \ n = 0, 1, 2, \cdots.$$

Thus, we have

$$\lambda_{1,n} = -d_1\frac{n^2}{l^2} + r_0 - d, \ \ \lambda_{2,n} = -d_2\frac{n^2}{l^2} - m, \ \ n = 0, 1, 2, \cdots.$$

Obviously, $\lambda_{2,n} < 0$. If $r_0 < d$, $\lambda_{1,n} < 0$ for all $n \in \mathbb{N}_0$, and if $r_0 > d$, $\lambda_{1,0} > 0$. Thus, if $r_0 < d$, E_0 is locally asymptotically stable. If $r_0 > d$, E_0 is unstable.

If $r_0 > d$, the predator-free equilibrium $E_u(\frac{r_0-d}{a}, 0)$ exists. The corresponding characteristic equation is given by

$$(\lambda + d_1\frac{n^2}{l^2} + r_0 - d)(\lambda + d_2\frac{n^2}{l^2} + m - \frac{cp(r_0-d)}{(1+c_1k)[a+q(r_0-d)]}) = 0, \ \ n = 0, 1, 2, \cdots.$$

Since $r_0 - d > 0$, $\lambda_{1,n} = -d_1\frac{n^2}{l^2} - (r_0 - d) < 0$. Now we consider the sign of $\lambda_{2,n} = -[d_2\frac{n^2}{l^2} + m - \frac{cp(r_0-d)}{(1+c_1k)[a+q(r_0-d)]}]$. If (H1) holds, $\lambda_{2,0} = -m + \frac{cp(r_0-d)}{(1+c_1k)[a+q(r_0-d)]} > 0$, which indicates that E_u is unstable. If $\frac{m(1+c_1k)}{pc-mq(1+c_1k)} > \frac{r_0-d}{a} > 0$ holds, $\lambda_{2,n} < 0$ for all $n \in \mathbb{N}_0$, and E_u is locally asymptotically stable.

Theorem 1. *(i) When $r_0 < d$, there is only the trivial equilibrium E_0 for system (1.3), which is locally asymptotically stable; when $r_0 > d$, E_0 is unstable and there is a predator-free equilibrium E_u.*

(ii) When $\frac{m(1+c_1k)}{pc-mq(1+c_1k)} > \frac{r_0-d}{a} > 0$, E_u is locally asymptotically stable; When (H1) *holds, E_u is unstable and there is a positive equilibrium E^*.*

For the positive equilibrium $E^*(u^*, v^*)$ of system (1.3), we have

$$\begin{aligned} &J_{11} = -au^* + \tfrac{pqu^*v^*}{(1+c_1k)(1+qu^*)^2}, \quad J_{12} = -\tfrac{pu^*}{(1+c_1k)(1+qu^*)} < 0, \\ &J_{21} = \tfrac{cpv^*}{(1+c_1k)(1+qu^*)^2} > 0, \quad J_{22} = 0, \quad K_{12} = -\tfrac{r_0c_2ku^*}{(1+c_2kv^*)^2} < 0. \end{aligned} \tag{2.5}$$

The characteristic equation becomes

$$\lambda^2 + T_n\lambda + D_n + Me^{-\lambda\tau} = 0, \quad n = 0, 1, 2, \cdots, \tag{2.6}$$

where

$$\begin{aligned} T_n &= (d_1 + d_2)\frac{n^2}{l^2} - J_{11}, \\ D_n &= d_1 d_2 \frac{n^4}{l^4} - J_{11} d_2 \frac{n^2}{l^2} - J_{21}J_{12}, \\ M &= -J_{21}K_{12} > 0. \end{aligned}$$

When $\tau = 0$, the characteristic equation (2.6) becomes

$$\lambda^2 + T_n\lambda + D_n + M = 0, \quad n = 0, 1, 2, \cdots. \tag{2.7}$$

Obviously, $D_0 + M = -J_{21}J_{12} - J_{21}K_{12} > 0$. Hence, if

$$\text{(H2)} \quad J_{11} = -au^* + \frac{pqu^*v^*}{(1 + c_1k)(1 + qu^*)^2} < 0$$

holds, we have $T_n > 0$, $D_n + M > 0$ for all $n \in \mathbb{N}_0$, thus all roots of Eq (2.7) have negative real parts. If $J_{11} > 0$, we have $T_0 < 0$ and $D_0 + M > 0$, the roots of (2.7) have positive real parts when $n = 0$, which means that E^* is unstable in the absence of diffusion. To sum up, Turing instability induced by diffusion will not occur.

In the following, we assume that (H2) always holds, which ensures $T_n > 0$, $D_n > 0$ and $D_n + M > 0$. Thus, a change of stability at $E^*(u^*, v^*)$ can only happen when there is at least one root of Eq (2.6) across the imaginary axis on the complex plane. After excluding Turing instability induced by diffusion, now we seek the critical values of τ where the roots of Eq (2.6) will cross the imaginary axis from the left half plane to the right half plane. Plugging $\lambda = \mathrm{i}\omega_n(\omega_n > 0)$ into Eq (2.6), we obtain

$$-\omega_n^2 + T_n\mathrm{i}\omega_n + D_n + M(\cos\omega_n\tau - \mathrm{i}\sin\omega_n\tau) = 0.$$

Separating the real and imaginary parts, we obtain

$$\begin{cases} \cos(\omega_n\tau) = \frac{\omega_n^2 - D_n}{M} = C_n(\omega_n), \\ \sin(\omega_n\tau) = \frac{T_n\omega_n}{M} = S_n(\omega_n). \end{cases} \tag{2.8}$$

Squaring and adding both equations of (2.8), we have

$$\omega_n^4 + (T_n^2 - 2D_n)\omega_n^2 + D_n^2 - M^2 = 0. \tag{2.9}$$

The number of positive roots of Eq (2.9) is relevant to the signs of $T_n^2 - 2D_n$ and $D_n^2 - M^2$. For the convenience of discussion, we make the following assumptions.

$$\begin{aligned} &\text{(H3)} \quad T_0^2 - 2D_0 \geq 0 \text{ and } D_0 - M \geq 0. \\ &\text{(H4)} \quad T_0^2 - 2D_0 < 0 \text{ and } D_0 - M > 0. \\ &\text{(H5)} \quad T_0^2 - 2D_0 < 0 \text{ and } D_0 - M = 0. \\ &\text{(H6)} \quad T_0^2 - 2D_0 \geq 0 \text{ and } D_0 - M < 0. \\ &\text{(H7)} \quad T_0^2 - 2D_0 < 0 \text{ and } D_0 - M < 0. \end{aligned}$$

Before the discussion of these cases, we need to investigate some properties of $T_n^2 - 2D_n$ and $D_n^2 - M^2$.

Lemma 1. *Suppose that* (H1) *and* (H2) *hold.* $T_n^2 - 2D_n$ *and* $D_n^2 - M^2$ *are both monotonically increasing with respect to n.*

Proof. When (H2) holds, we have

$$\frac{\mathrm{d}(T_n^2 - 2D_n)}{\mathrm{d}n} = 2\left(T_n\frac{\mathrm{d}T_n}{\mathrm{d}n} - \frac{\mathrm{d}D_n}{\mathrm{d}n}\right) = 2\left(d_1^2\frac{2n^3}{l^4} + d_2^2\frac{2n^3}{l^4} - J_{11}d_1\frac{2n}{l^2}\right) > 0,$$

which means that $T_n^2 - 2D_n$ is monotonically increasing with respect to n. Similarly, when $J_{11} < 0$, we have $D_n > 0$, and

$$\frac{\mathrm{d}(D_n^2 - M^2)}{\mathrm{d}n} = 2D_n\frac{\mathrm{d}D_n}{\mathrm{d}n} = 2D_n\left(d_1d_2\frac{4n^3}{l^4} - J_{11}d_2\frac{2n}{l^2}\right) > 0.$$

□

2.1. *Case I when* (H3) *holds*

We first consider the case when (H3) holds.

Lemma 2. *If* (H1)*,* (H2) *and* (H3) *hold, then all roots of Eq (2.6) have negative real parts for all* $\tau \geq 0$*.*

Proof. Noticing that $D_n + M > 0$ for all $n \in \mathbb{N}_0$, thus $D_0 - M \geq 0$ leads to $D_0^2 - M^2 \geq 0$. From Lemma 1 and (H3), we can deduce that $T_n^2 - 2D_n \geq 0$ and $D_n^2 - M^2 \geq 0$ for all $n \in \mathbb{N}_0$. Therefore, Eq (2.9) has no positive roots, and Eq (2.6) has no imaginary roots. □

Theorem 2. *If* (H1)*,* (H2) *and* (H3) *hold, the positive equilibrium* E^* *is locally asymptotically stable for all* $\tau \geq 0$*.*

2.2. *Case II when* (H4) *holds*

Lemma 3. *If* (H1)*,* (H2) *and* (H4) *hold, there exists* $n_1 \in \mathbb{N}_0$ *such that the following conclusions hold.*

(i) If either $n > n_1$ *or* $0 \leq n \leq n_1$ *and* $\Delta = (T_n^2 - 2D_n)^2 - 4(D_n^2 - M^2) < 0$*, then all roots of Eq (2.6) have negative real parts for all* $\tau \geq 0$*.*

(ii) If $\Delta > 0$ *for* $0 \leq n \leq n_1$ *, then Eq (2.6) has a pair of imaginary roots* $\pm\mathrm{i}\omega_n^+(\pm\mathrm{i}\omega_n^-,$ respectively*) for* $0 \leq n \leq n_1$*.*

Proof. Similar as the proof in Lemma 2, we have $D_n^2 - M^2 > 0$ for all $n \in \mathbb{N}_0$. When $T_0^2 - 2D_0 < 0$, from Lemma 1, there exists $n_1 \in \mathbb{N}_0$ such that

$$\begin{cases} T_n^2 - 2D_n \geq 0, & n > n_1, \\ T_n^2 - 2D_n < 0, & 0 \leq n \leq n_1. \end{cases} \tag{2.10}$$

It means that Eq (2.9) has no positive roots for $n > n_1$. For $0 \leq n \leq n_1$, if $\Delta = (T_n^2 - 2D_n)^2 - 4(D_n^2 - M^2) < 0$, Eq (2.9) has no positive roots, and if $\Delta > 0$, Eq (2.9) has two positive roots $\omega_n^{\pm}$, where

$$\omega_n^{\pm} = [\frac{1}{2}(2D_n - T_n^2 \pm \sqrt{\Delta})]^{\frac{1}{2}}. \tag{2.11}$$

Correspondingly, Eq (2.6) has a pair of purely imaginary roots $\pm\mathrm{i}\omega_n^+(\pm\mathrm{i}\omega_n^-,$ respectively) for $0 \leq n \leq n_1$. □

Since (H2) holds, we have $T_n > 0$. Noticing that $M = -J_{21}K_{12} > 0$, from (2.8), we have $S_n(\omega_n^{\pm}) > 0$, and we get

$$\tau_n^{j\pm} = \frac{1}{\omega_n^{\pm}}(\arccos[\frac{(\omega_n^{\pm})^2 - D_n}{M}] + 2j\pi), \quad 0 \le n \le n_1, \quad j = 0, 1, 2, \cdots . \tag{2.12}$$

Lemma 4. *Assume that* (H1)*,* (H2) *and* (H4) *hold. If* $\Delta > 0$*, then* $\mathrm{Re}\left[\frac{\mathrm{d}\lambda}{\mathrm{d}\tau}\right]_{\tau=\tau_n^{j+}} > 0$*,* $\mathrm{Re}\left[\frac{\mathrm{d}\lambda}{\mathrm{d}\tau}\right]_{\tau=\tau_n^{j-}} < 0$*, for* $0 \le n \le n_1$*,* $j = 0, 1, 2, \cdots$*, where* n_1 *is defined in (2.10).*

Proof. Differentiating two sides of (2.6) with respect to τ, we obtain

$$\mathrm{Re}\left[\frac{\mathrm{d}\lambda}{\mathrm{d}\tau}\right]^{-1}_{\tau=\tau_n^{j\pm}} = \frac{2\omega_n^{\pm}\cos(\omega_n^{\pm}\tau) + T_n\sin(\omega_n^{\pm}\tau)}{M\omega_n^{\pm}} = \frac{2\omega_n^{\pm}(\omega_n^{\pm^2} - D_n) + T_n^2\omega_n^{\pm}}{M^2\omega_n^{\pm}} = \pm\frac{\sqrt{\Delta}}{M^2}.$$

The sign of $\mathrm{Re}\left[\frac{\mathrm{d}\lambda}{\mathrm{d}\tau}\right]_{\tau=\tau_n^{j\pm}}$ is the same as that of $\mathrm{Re}\left[\frac{\mathrm{d}\lambda}{\mathrm{d}\tau}\right]^{-1}_{\tau=\tau_n^{j\pm}}$, thus we have $\mathrm{Re}\left[\frac{\mathrm{d}\lambda}{\mathrm{d}\tau}\right]_{\tau=\tau_n^{j+}} > 0$, $\mathrm{Re}\left[\frac{\mathrm{d}\lambda}{\mathrm{d}\tau}\right]_{\tau=\tau_n^{j-}} < 0$. □

Now we consider the order of the critical values Hopf bifurcation.

Lemma 5. *Assume that* (H1)*,* (H2) *and* (H4) *hold, and* $\Delta > 0$ *for* $0 \le n \le n_1$*.* τ_n^{j+} *is monotonically increasing and* τ_n^{j-} *is monotonically decreasing with respect to n (*$0 < n \le n_1$*), where* n_1 *and* $\tau_n^{j\pm}$ *are defined in (2.10) and (2.12), respectively.*

Proof. See Appendix A. □

Theorem 3. *Assume that* (H1)*,* (H2) *and* (H4) *hold, and* n_1 *is defined in (2.10).*

(i) If $\Delta < 0$ *for* $0 \le n \le n_1$*,* E^* *is locally asymptotically stable for all* $\tau > 0$*.*

(ii) If $\Delta > 0$ *for* $0 \le n \le n_1$*, system (1.3) undergoes a Hopf bifurcation at* E^* *when* $\tau = \tau_n^{j\pm}$ $(0 \le n \le n_1,\ j = 0, 1, 2, \cdots)$*. Moreover,* E^* *is locally asymptotically stable when* $\tau \in [0, \tau_0^{0+}) \cup (\tau_0^{0-}, \tau_0^{1+}) \cup \cdots \cup (\tau_0^{(s-1)-}, \tau_0^{s+})$*, and it is unstable when* $\tau \in (\tau_0^{0+}, \tau_0^{0-}) \cup (\tau_0^{1+}, \tau_0^{1-}) \cup \cdots \cup (\tau_0^{s+}, +\infty)$*.*

Proof. (i) From Lemma 3, when $\Delta < 0$, Eq (2.6) has no purely imaginary roots, thus the stability of E^* can not be changed by delay.

(ii) When $\Delta > 0$, from Lemma 5, we have $\tau_0^{j+} < \tau_1^{j+} < \cdots < \tau_{n_1}^{j+}$, and $\tau_{n_1}^{j-} < \cdots < \tau_0^{j-}$, $j = 0, 1, 2, \cdots$. From $\omega_{n_1}^{+} > \omega_{n_1}^{-}$, we have $\arccos\left[\frac{(\omega_{n_1}^{+})^2 - D_{n_1}}{M}\right] < \arccos\left[\frac{(\omega_{n_1}^{-})^2 - D_{n_1}}{M}\right]$, and $\tau_{n_1}^{j+} < \tau_{n_1}^{j-}$. Therefore, $\tau_0^{j+} < \cdots < \tau_{n_1}^{j+} < \tau_{n_1}^{j-} < \cdots < \tau_0^{j-}$.

We claim that there exists a positive integer s such that $\tau_0^{0+} < \tau_0^{0-} < \tau_0^{1+} < \tau_0^{1-} < \cdots < \tau_0^{s+} < \tau_0^{(s+1)+} < \tau_0^{s-}$. Since $\omega_0^{-} < \omega_0^{+}$, $\tau_0^{j+} - \tau_0^{(j-1)+} = \frac{2\pi}{\omega_0^{+}} < \tau_0^{j-} - \tau_0^{(j-1)-} = \frac{2\pi}{\omega_0^{-}}$, which means that the alternation for τ_0^{j+} and τ_0^{j-} cannot persist for the entire sequence, and there exists a positive integer s such that $\tau_0^{(s-1)+} < \tau_0^{(s-1)-} < \tau_0^{s+} < \tau_0^{(s+1)+} < \tau_0^{s-}$. From Lemma 4, we can get the stable and unstable interval for τ.

□

2.3. Case III when (H5)*,* (H6) *or* (H7) *holds*

First, we consider the case when (H5) holds. If (H5) holds, Eq (2.9) has a positive root $\omega_0^+ = 2D_0 - T_0^2$ when $n = 0$. Similar as Lemma 3, there exists $n_1 \in \mathbb{N}_0$ such that (2.10) holds. If $\Delta > 0$ for $0 < n \le n_1$, Eq (2.6) has a pair of imaginary roots $\pm i\omega_n^+(\pm i\omega_n^-$, respectively) for $0 < n \le n_1$.

Lemma 6. *If* (H1)*,* (H2) *and* (H5) *hold, there exists* $n_1 \in \mathbb{N}_0$ *defined in (2.10).*

(i) If either $n > n_1$ *or* $0 < n \le n_1$ *and* $\Delta < 0$*, then all roots of Eq (2.6) have negative real parts for all* $\tau \ge 0$*.*
(ii) If $n = 0$*, then Eq (2.6) has a pair of imaginary roots* $\pm i\omega_0^+$*.*
(iii) If $\Delta > 0$ *for* $0 < n \le n_1$ *, then Eq (2.6) has a pair of imaginary roots* $\pm i\omega_n^+(\pm i\omega_n^-$, respectively) *for* $0 < n \le n_1$*.*

Remark 1. *Similar as the proof of Lemma 5 and Theorem 3, we can get* $\tau_0^{j+} < \tau_1^{j+} < \cdots < \tau_{n_1}^{j+} < \tau_{n_1}^{j-} < \cdots < \tau_1^{j-}$*, where* $\tau_n^{j\pm}$ *is defined in (2.12). Similar as Lemma 4, we can verify that* $\mathrm{Re}\left[\frac{d\lambda}{d\tau}\right]_{\tau=\tau_n^{j+}} > 0$ *for* $0 \le n \le n_1$ *and* $\mathrm{Re}\left[\frac{d\lambda}{d\tau}\right]_{\tau=\tau_n^{j-}} < 0$ *for* $0 < n \le n_1$*. Being different from case II, stability switches can not happen.*

Now we consider the case when (H6) holds. From Lemma 1, and $T_0^2 - 2D_0 \ge 0$, we have $T_n^2 - 2D_n \ge 0$ for all $n \in \mathbb{N}_0$. From Lemma 1, combining $D_0 - M < 0$ with $D_n + M > 0$, we get

$$D_n^2 - M^2 \begin{cases} \ge 0, & n > n_2, \\ \\ < 0, & 0 \le n \le n_2. \end{cases} \tag{2.13}$$

Equation (2.9) has only one positive root ω_n^+ for $0 \le n \le n_2$, where

$$\omega_n^+ = [\frac{1}{2}(2D_n - T_n^2 + \sqrt{\Delta})]^{\frac{1}{2}}.$$

Lemma 7. *Assume that* (H1)*,* (H2) *and* (H6) *hold, and* $n_2 \in \mathbb{N}_0$ *is defined in (2.13).*

(i) If $n > n_2$*, then all roots of Eq (2.6) have negative real parts for all* $\tau \ge 0$*.*
(ii) If $0 \le n \le n_2$ *, then Eq (2.6) has a pair of imaginary roots* $\pm i\omega_n^+$ *for* $0 \le n \le n_2$*.*

It is easy to get $S_n(\omega_n^+) > 0$, from (2.8), we have

$$\tau_n^{j+} = \frac{1}{\omega_n^+}(\arccos[\frac{(\omega_n^+)^2 - D_n}{M}] + 2j\pi), \quad 0 \le n \le n_2, \quad j = 0, 1, 2, \cdots. \tag{2.14}$$

When (H7) holds, from Lemma 1, we can deduce that there exists n_1 and n_2 such that

$$T_n^2 - 2D_n \begin{cases} \ge 0, & n > n_1, \\ \\ < 0, & 0 \le n \le n_1, \end{cases} \qquad D_n^2 - M^2 \begin{cases} \ge 0, & n > n_2, \\ \\ < 0, & 0 \le n \le n_2. \end{cases} \tag{2.15}$$

If $n_1 \le n_2$, Eq (2.9) has only one positive root ω_n^+ for $0 \le n \le n_2$, where

$$\tau_n^{j+} = \frac{1}{\omega_n^+}(\arccos C_n(\omega_n^+) + 2j\pi), \quad 0 \le n \le n_2, \quad j = 0, 1, 2, \cdots,$$

and Eq (2.9) has no positive roots for $n > n_2$.

If $n_2 \le n_1$, Eq (2.9) has one positive root ω_n^+ for $0 \le n \le n_2$, and has two positive roots $\omega_n^\pm$ for $n_2 + 1 < n \le n_1$, and has no positive roots for $n > n_1$. When $n = n_2 + 1$, if $D_{n_2+1}^2 - M^2 > 0$, Eq (2.9) has two positive roots $\omega_{n_2+1}^\pm$, and if $D_{n_2+1}^2 - M^2 = 0$, Eq (2.9) has one positive root $\omega_{n_2+1}^+$. Similar as the proof in Lemma 5, we have

$$\begin{cases} \tau_0^{j+} < \cdots < \tau_{n_2}^{j+} < \tau_{n_2+1}^{j+} < \cdots < \tau_{n_1}^{j+} < \tau_{n_1}^{j-} < \cdots < \tau_{n_2+2}^{j-} < \tau_{n_2+1}^{j-}, & \text{if } D_{n_2+1}^2 - M^2 > 0, \\ \tau_0^{j+} < \cdots < \tau_{n_2}^{j+} < \tau_{n_2+1}^{j+} < \cdots < \tau_{n_1}^{j+} < \tau_{n_1}^{j-} < \cdots < \tau_{n_2+2}^{j-}, & \text{if } D_{n_2+1}^2 - M^2 = 0, \end{cases}$$

where

$$\begin{cases} \tau_n^{j+} = \dfrac{1}{\omega_n^+}(\arccos C_n(\omega_n^+) + 2j\pi), \quad 0 \le n \le n_2, \quad j = 0, 1, 2, \cdots, \\ \tau_n^{j\pm} = \dfrac{1}{\omega_n^\pm}(\arccos C_n(\omega_n^\pm) + 2j\pi), \quad n_2 + 1 < n \le n_1, \quad j = 0, 1, 2, \cdots, \\ \tau_{n_2+1}^{j+} = \begin{cases} \frac{1}{\omega_{n_2+1}^\pm}(\arccos C_{n_2+1}(\omega_{n_2+1}^\pm) + 2j\pi), & \text{if } D_{n_2+1}^2 - M^2 > 0, \quad j = 0, 1, 2, \cdots, \\ \frac{1}{\omega_{n_2+1}^+}(\arccos C_{n_2+1}(\omega_{n_2+1}^+) + 2j\pi), & \text{if } D_{n_2+1}^2 - M^2 = 0, \quad j = 0, 1, 2, \cdots. \end{cases} \end{cases}$$

For either $n_1 \le n_2$ or $n_2 \le n_1$, we have

$$\tau_0^{0+} = \min\{\tau_n^{j\pm} \text{ or } \tau_n^{j+} \mid 0 \le n \le \max\{n_1, n_2\}, \ j = 0, 1, 2, \cdots\}. \tag{2.16}$$

From the previous discussion, we can get the following conclusions.

Theorem 4. *Assume that* (H1) *and* (H2) *hold, and n_1, n_2 are defined in (2.15). If* (H5), (H6) *or* (H7) *holds, E^* is locally asymptotically stable when $\tau \in [0, \tau_0^{0+})$, and E^* is unstable when $\tau > \tau_0^{0+}$.*

Proof. If (H5), (H6) or (H7) holds, we easily know that τ_0^{0+} is the smallest critical value of Hopf bifurcation values. Similar as Lemma 4, we can get the transversality condition, which can lead to the results. □

3. Double Hopf bifurcation

In order to figure out the joint effect of fear level k and fear response delay τ on the dynamical behavior of system (1.3), we carry out double Hopf bifurcation analysis. We first verify the condition for the occurrence of double Hopf bifurcation.

Remark 2. *Assume that* (H1), (H2) *and* (H4) *hold. If there exists $k = k^*$ such that $\tau_{n_1}^{j_1+} = \tau_{n_2}^{j_2-} = \tau^*$. Then system (1.3) may undergo a double Hopf bifurcation at the positive equilibrium $E^*(u^*, v^*)$ when $(k, \tau) = (k^*, \tau^*)$.*

Define the real-valued Hilbert space $X := \left\{(u, v) \in H^2(0, l\pi) \times H^2(0, l\pi) : (u_x, v_x)\big|_{x=0,l\pi} = 0\right\}$, and the corresponding complex space $X_{\mathbb{C}} := \{x_1 + \mathrm{i}x_2, x_1, x_2 \in X\}$. Let $\widetilde{u} = u(x, \tau t) - u^*$, $\widetilde{v} = v(x, \tau t) - v^*$, and drop the hats for the convenience of notation. Denote $U(t) = (u(x, t), v(x, t))^T$, and $U_t(\theta) = U(t + \theta)$, $-1 \le \theta \le 0$. System (1.3) can be written as

$$\begin{aligned} \frac{\mathrm{d}U}{\mathrm{d}t} &= \tau D\Delta U(t) + \tau[G_0(k)U_t(0) + G_1(k)U_t(-1)] + \tau[\frac{1}{2!}(F_{uu}u_t^2(0) + 2F_{uv}u_t(0)v_t(0) + F_{v_tv_t}v_t^2(-1) \\ &\quad + 2F_{uv_t}u_t(0)v_t(-1)) + \frac{1}{3!}(F_{uuu}u_t^3(0) + 3F_{uuv}u_t^2(0)v_t(0) + 3F_{uv_tv_t}u_t(0)v_t^2(-1) + F_{v_tv_tv_t}v_t^3(-1))], \end{aligned} \tag{3.1}$$

where the coefficients of nonlinear terms F_{uu}, F_{uv}, etc., are in Appendix B, and

$$G_0(k) = \begin{pmatrix} J_{11}(k) & J_{12}(k) \\ J_{21}(k) & 0 \end{pmatrix}, \ G_1(k) = \begin{pmatrix} 0 & K_{12}(k) \\ 0 & 0 \end{pmatrix}.$$

Here $J_{11}(k), J_{12}(k), J_{21}(k)$, and $K_{12}(k)$ are defined in (2.5), in which u^*, v^* are functions of k defined in (2.1).

Let $k = k^* + \alpha_1$, $\tau = \tau^* + \alpha_2$, then $(\alpha_1, \alpha_2) = (0, 0)$ is a double Hopf bifurcation point. System (3.1) can be written as

$$\frac{\mathrm{d}U}{\mathrm{d}t} = D_0\Delta U(t) + L_0U_t + \widetilde{F}(\alpha_1, \alpha_2, U_t), \tag{3.2}$$

where

$$\begin{aligned} &D_0 = \tau^*D, \quad L_0U_t = \tau^*(G_0(k^*)U_t(0) + G_1(k^*)U_t(-1)), \\ &\widetilde{F}(\alpha_1, \alpha_2, U_t) = \frac{1}{2!}F_2(\alpha_1, \alpha_2, U_t) + \frac{1}{3!}F_3(\alpha_1, \alpha_2, U_t) + \cdots, \end{aligned}$$

with

$$\begin{aligned} F_2(\alpha_1, \alpha_2, U_t) &= 2((\alpha_1D_1^{(1,0)} + \alpha_2D_1^{(0,1)})\Delta U + \alpha_1L_1^{(1,0)}U_t + \alpha_2L_1^{(0,1)}U_t) \\ &\quad + 2F_{uv}u_t(0)v_t(0) + F_{uu}u_t^2(0) + 2F_{uv_t}u_t(0)v_t(-1) + F_{v_tv_t}v_t^2(-1), \\ F_3(0, 0, U_t) &= F_{v_tv_tv_t}v_t^3(-1) + 3F_{uuv}u_t^2(0)v_t(0) + 3F_{uv_tv_t}u_t(0)v_t^2(-1) + F_{uuu}u_t^3(0), \end{aligned}$$

and

$$\begin{aligned} &D_1^{(1,0)} = 0, \ \ D_1^{(0,1)} = D, \ \ L_1^{(0,1)}U_t = G_0(k^*)U_t(0) + G_1(k^*)U_t(-1), \\ &L_1^{(1,0)}U_t = \tau^*\begin{pmatrix} J_{11}'(k^*) & J_{12}'(k^*) \\ J_{21}'(k^*) & 0 \end{pmatrix}U_t(0) + \tau^*\begin{pmatrix} 0 & K_{12}'(k^*) \\ 0 & 0 \end{pmatrix}U_t(-1). \end{aligned}$$

We leave the detailed calculation and some expressions in Appendix C.

Define an enlarged phase space $\mathcal{BC}$ by

$$\mathcal{BC} := \{\psi : [-1, 0] \to X_{\mathbb{C}} : \psi \text{ is continuous on} [-1, 0), \exists \lim_{\theta\to 0^-} \psi(\theta) \in X_{\mathbb{C}}\}.$$

Equation (3.2) can be written as an abstract ordinary differential equation in $\mathcal{BC}$

$$\frac{\mathrm{d}U_t}{\mathrm{d}t} = AU_t + X_0\widetilde{F}(\alpha_1, \alpha_2, U_t), \tag{3.3}$$

where $A\varphi = \dot{\varphi} + X_0[D_0\Delta\varphi(0) + L_0(\varphi) - \dot{\varphi}(0)]$, with

$$X_0(\theta) = \begin{cases} 0, & -1 \le \theta < 0, \\ I_2, & \theta = 0. \end{cases}$$

It is obvious that $\{\pm\mathrm{i}\omega_{n_1}^+\tau^*, \pm\mathrm{i}\omega_{n_2}^-\tau^*\}$ are the pure imaginary eigenvalues of the operator A and the corresponding eigenfunctions in $\mathcal{BC}$ are $\{\phi_1(\theta)\gamma_{n_1}, \phi_2(\theta)\gamma_{n_1}, \phi_3(\theta)\gamma_{n_2}, \phi_4(\theta)\gamma_{n_2}\}$, respectively, where

$$\gamma_n(x) = \frac{\cos\frac{n}{l}x}{\| \cos\frac{n}{l}x \|_{L^2}} = \begin{cases} \sqrt{\frac{1}{l\pi}}, & n = 0, \\ \sqrt{\frac{2}{l\pi}}\cos\frac{n}{l}x, & n \ge 1, \end{cases}$$

and $\phi_1(\theta) = (1, p_{12})^T e^{i\omega^+_{n_1}\tau^*\theta}$, $\phi_3(\theta) = (1, p_{32})^T e^{i\omega^-_{n_2}\tau^*\theta}$, $\phi_2(\theta) = \overline{\phi_1(\theta)}$, $\phi_4(\theta) = \overline{\phi_3(\theta)}$, with

$$p_{12} = \frac{-J_{11}(k^*) + \frac{n_1^2}{l^2}d_1 + i\omega^+_{n_1}}{J_{12}(k^*) + K_{12}(k^*)e^{-i\omega^+_{n_1}\tau^*}}, \quad p_{32} = \frac{-J_{11}(k^*) + \frac{n_2^2}{l^2}d_1 + i\omega^-_{n_2}}{J_{12}(k^*) + K_{12}(k^*)e^{-i\omega^-_{n_2}\tau^*}}.$$

A direct calculation derived that $\psi_1(s) = D_1(1, q_{12})e^{-i\omega^+_{n_1}\tau^* s}$, $\psi_3(s) = D_3(1, q_{32})e^{-i\omega^-_{n_2}\tau^* s}$ are the formal adjoint eigenvectors of $\phi_1(\theta)$, $\phi_3(\theta)$ and satisfy $(\phi_1, \psi_1)_1 = 1$, $(\phi_3, \psi_3)_2 = 1$. Here

$$q_{12} = \frac{-J_{11}(k^*) + \frac{n_1^2}{l^2}d_1 + i\omega^+_{n_1}}{J_{21}(k^*)}, \qquad q_{32} = \frac{-J_{11}(k^*) + \frac{n_2^2}{l^2}d_1 + i\omega^-_{n_2}}{J_{21}(k^*)},$$
$$D_1 = (1 + p_{12}q_{12} + \tau^* K_{12}(k^*)p_{12}e^{-i\omega^+_{n_1}\tau^*})^{-1}, \quad D_3 = (1 + p_{32}q_{32} + \tau^* K_{12}(k^*)p_{32}e^{-i\omega^-_{n_2}\tau^*})^{-1},$$

and $(\cdot, \cdot)_k$ are the adjoint bilinear form

$$(\psi, \phi)_k = \psi(0)\phi(0) - \int_{-1}^{0}\int_{\xi=0}^{\theta} \psi(\xi - \theta)d\eta_k(\theta, \tau^*)\phi(\xi)d\xi, \quad k = 1, 2,$$

with a function of bounded variation $\eta_k(\theta, \tau^*)$, $\theta \in [-1, 0]$ are given by

$$-D_0\frac{n_k^2}{l^2}\phi(0) + L_0(\phi) = \int_{-1}^{0} d\eta_k(\theta, \tau^*)\phi(\theta), \ \phi \in C, \quad k = 1, 2.$$

Denote

$$\Phi_1(\theta) = (\phi_1(\theta), \phi_2(\theta)), \quad \Phi_2(\theta) = (\phi_3(\theta), \phi_4(\theta)),$$
$$\Psi_1(s) = (\psi_1(s), \psi_2(s))^T, \ \Psi_2(s) = (\psi_3(s), \psi_4(s))^T,$$

where $\psi_2(s) = \overline{\psi_1(s)}$, $\psi_4(s) = \overline{\psi_3(s)}$.

Now we decompose $\mathcal{BC}$ into the direct sum of the central subspace $\mathcal{P}$ and its complementary space Kerπ

$$\mathcal{BC} = \mathcal{P} \oplus \text{Ker}\pi, \tag{3.4}$$

where $\pi : \mathcal{BC} \to \mathcal{P}$ is the projection defined by

$$\pi(\varphi) = \sum_{k=1}^{2} \Phi_k(\Psi_k, \langle\varphi(\cdot), \beta_{n_k}\rangle)_k \cdot \beta_{n_k}.$$

According to (3.4), U_t can be decomposed as

$$U_t(\theta) = \phi_1(\theta)z_1(t)\gamma_{n_1} + \phi_2(\theta)z_2(t)\gamma_{n_1} + \phi_3(\theta)z_3(t)\gamma_{n_2} + \phi_4(\theta)z_4(t)\gamma_{n_2} + y_t(\theta),$$

where $(z_1, z_2, z_3, z_4)^T = (\tilde{z}_1, \tilde{z}_2) = (\Psi_k, \langle U_t, \beta_{n_k}\rangle)_k$, and $y_t(\theta) \in \text{Ker}\pi$.

Then system (3.3) in $\mathcal{BC}$ is equivalent to the system

$$\begin{cases} \dot{z}_1 &= i\omega^+_{n_1}\tau^* z_1 + \psi_1(0)\langle\frac{1}{2!}\widetilde{F}_2(z, y, \alpha) + \frac{1}{3!}\widetilde{F}_3(z, y, \alpha), \beta_{n_1}\rangle + \cdots, \\ \dot{z}_2 &= -i\omega^+_{n_1}\tau^* z_2 + \psi_2(0)\langle\frac{1}{2!}\widetilde{F}_2(z, y, \alpha) + \frac{1}{3!}\widetilde{F}_3(z, y, \alpha), \beta_{n_1}\rangle + \cdots, \\ \dot{z}_3 &= i\omega^-_{n_2}\tau^* z_3 + \psi_3(0)\langle\frac{1}{2!}\widetilde{F}_2(z, y, \alpha) + \frac{1}{3!}\widetilde{F}_3(z, y, \alpha), \beta_{n_2}\rangle + \cdots, \\ \dot{z}_4 &= -i\omega^-_{n_2}\tau^* z_4 + \psi_4(0)\langle\frac{1}{2!}\widetilde{F}_2(z, y, \alpha) + \frac{1}{3!}\widetilde{F}_3(z, y, \alpha), \beta_{n_2}\rangle + \cdots, \\ \frac{dy}{dt} &= A_1 y + (I - \pi)X_0[\frac{1}{2!}\widetilde{F}_2(z, y, \alpha) + \frac{1}{3!}\widetilde{F}_3(z, y, \alpha)], \end{cases}$$

where A_1 is the restriction of A on $Q^1 \subset \mathrm{Ker}\pi \to \mathrm{Ker}\pi$, $A_1\varphi = A\varphi$ for $\varphi \in Q^1$, and $\widetilde{F}_2(z, y, \alpha)$ and $\widetilde{F}_3(z, 0, 0)$ are in Appendix D.

According to [28], we can obtain the normal form of the double Hopf bifurcation up to the third order as follows

$$\begin{aligned}
\dot{z}_1 &= \mathrm{i}\omega_{n_1}^+\tau^* z_1 + B_{11}\alpha_1 z_1 + B_{21}\alpha_2 z_1 + B_{2100}z_1^2 z_2 + B_{1011}z_1 z_3 z_4,\\
\dot{z}_2 &= -\mathrm{i}\omega_{n_1}^+\tau^* z_2 + \overline{B_{11}}\alpha_1 z_2 + \overline{B_{21}}\alpha_2 z_2 + \overline{B_{2100}}z_1 z_2^2 + \overline{B_{1011}}z_2 z_3 z_4,\\
\dot{z}_3 &= \mathrm{i}\omega_{n_2}^-\tau^* z_3 + B_{13}\alpha_1 z_3 + B_{23}\alpha_2 z_3 + B_{0021}z_3^2 z_4 + B_{1110}z_1 z_2 z_3,\\
\dot{z}_4 &= -\mathrm{i}\omega_{n_2}^-\tau^* z_4 + \overline{B_{13}}\alpha_1 z_4 + \overline{B_{23}}\alpha_2 z_4 + \overline{B_{0021}}z_3 z_4^2 + \overline{B_{1110}}z_1 z_2 z_4.
\end{aligned} \tag{3.5}$$

Here

$$\begin{aligned}
&B_{11} = \psi_1(0)\Big(-\frac{n_1^2}{l^2}D_1^{(1,0)}\phi_1(0) + L_1^{(1,0)}\phi_1\Big),\ B_{21} = \psi_1(0)\Big(-\frac{n_1^2}{l^2}D_1^{(0,1)}\phi_1(0) + L_1^{(0,1)}\phi_1\Big),\\
&B_{13} = \psi_3(0)\Big(-\frac{n_2^2}{l^2}D_1^{(1,0)}\phi_3(0) + L_1^{(1,0)}\phi_3\Big),\ B_{23} = \psi_3(0)\Big(-\frac{n_2^2}{l^2}D_1^{(0,1)}\phi_3(0) + L_1^{(0,1)}\phi_3\Big),\\
&B_{2100} = C_{2100} + \frac{3}{2}\left(D_{2100} + E_{2100}\right), \qquad B_{1011} = C_{1011} + \frac{3}{2}(D_{1011} + E_{1011}),\\
&B_{0021} = C_{0021} + \frac{3}{2}(D_{0021} + E_{0021}), \qquad B_{1110} = C_{1110} + \frac{3}{2}(D_{1110} + E_{1110}),
\end{aligned}$$

where

$$C_{2100} = \frac{1}{6l\pi}\psi_1(0)F_{2100},\ C_{1011} = \frac{1}{6l\pi}\psi_1(0)F_{1011},\ C_{0021} = \frac{1}{6l\pi}\psi_3(0)F_{0021},\ C_{1110} = \frac{1}{6l\pi}\psi_3(0)F_{1110},$$

$$\begin{aligned}
D_{2100} = \frac{1}{6\tau^*}\Big(&\frac{2}{-\mathrm{i}\omega_{n_1}^+}f_{2000}^{1(1)}f_{1100}^{1(1)} + \frac{1}{\mathrm{i}\omega_{n_1}^+}f_{1100}^{1(1)}f_{2000}^{1(1)} + \frac{1}{\mathrm{i}\omega_{n_1}^+}f_{1100}^{1(1)}f_{1100}^{1(2)}\\
&+ 2\frac{1}{3\mathrm{i}\omega_{n_1}^+}f_{0200}^{1(1)}f_{2000}^{1(2)} + \frac{1}{-\mathrm{i}\omega_{n_2}^-}f_{1010}^{1(1)}f_{1100}^{1(3)} + \frac{1}{2\mathrm{i}\omega_{n_1}^+ - \mathrm{i}\omega_{n_2}^-}f_{0110}^{1(1)}f_{2000}^{1(3)}\\
&+ \frac{1}{\mathrm{i}\omega_{n_2}^-}f_{1001}^{1(1)}f_{1100}^{1(4)} + \frac{1}{2\mathrm{i}\omega_{n_1}^+ + \mathrm{i}\omega_{n_2}^-}f_{0101}^{1(1)}f_{2000}^{1(4)}\Big),\\
D_{1011} = \frac{1}{6\tau^*}\Big(&\frac{2}{-\mathrm{i}\omega_{n_1}^+}f_{2000}^{1(1)}f_{0011}^{1(1)} + \frac{1}{-\mathrm{i}\omega_{n_2}^-}f_{1010}^{1(1)}f_{1001}^{1(1)} + \frac{1}{\mathrm{i}\omega_{n_2}^-}f_{1001}^{1(1)}f_{1010}^{1(1)} + \frac{1}{\mathrm{i}\omega_{n_1}^+}f_{1100}^{1(1)}f_{0011}^{1(2)}\\
&+ \frac{1}{2\mathrm{i}\omega_{n_1}^+ - \mathrm{i}\omega_{n_2}^-}f_{0110}^{1(1)}f_{1001}^{1(2)} + \frac{1}{2\mathrm{i}\omega_{n_1}^+ + \mathrm{i}\omega_{n_2}^-}f_{0101}^{1(1)}f_{1010}^{1(2)} + \frac{1}{-\mathrm{i}\omega_{n_2}^-}f_{1010}^{1(1)}f_{0011}^{1(3)}\\
&+ \frac{2}{\mathrm{i}\omega_{n_1}^+ - 2\mathrm{i}\omega_{n_2}^-}f_{0020}^{1(1)}f_{1001}^{1(3)} + \frac{1}{\mathrm{i}\omega_{n_1}^+}f_{0011}^{1(1)}f_{1010}^{1(3)} + \frac{1}{\mathrm{i}\omega_{n_2}^-}f_{1001}^{1(1)}f_{0011}^{1(4)}\\
&+ \frac{1}{\mathrm{i}\omega_{n_1}^+}f_{0011}^{1(1)}f_{1001}^{1(4)} + \frac{2}{\mathrm{i}\omega_{n_1}^+ + 2\mathrm{i}\omega_{n_2}^-}f_{0002}^{1(1)}f_{1010}^{1(4)}\Big),\\
D_{0021} = \frac{1}{6\tau^*}\Big(&\frac{2}{-\mathrm{i}\omega_{n_1}^+}f_{1010}^{1(3)}f_{0011}^{1(1)} + \frac{1}{2\mathrm{i}\omega_{n_2}^- - \mathrm{i}\omega_{n_1}^+}f_{1001}^{1(3)}f_{0020}^{1(1)} + \frac{1}{\mathrm{i}\omega_{n_1}^+}f_{0110}^{1(3)}f_{0011}^{1(2)}\\
&+ \frac{1}{2\mathrm{i}\omega_{n_2}^- + \mathrm{i}\omega_{n_1}^+}f_{0101}^{1(3)}f_{0020}^{1(2)} + 2\frac{1}{-\mathrm{i}\omega_{n_2}^-}f_{0020}^{1(3)}f_{0011}^{1(3)} + \frac{1}{\mathrm{i}\omega_{n_2}^-}f_{0011}^{1(3)}f_{0020}^{1(3)}\\
&+ \frac{1}{\mathrm{i}\omega_{n_2}^-}f_{0011}^{1(3)}f_{0011}^{1(4)} + 2\frac{1}{3\mathrm{i}\omega_{n_2}^-}f_{0002}^{1(3)}f_{0020}^{1(4)}\Big),
\end{aligned}$$

$$
\begin{aligned}
D_{1110} = & \frac{1}{6\tau^*}\Big(\frac{2}{-2\mathrm{i}\omega_{n_1}^{+}+\mathrm{i}\omega_{n_2}^{-}} f_{2000}^{1(3)} f_{0110}^{1(1)} + \frac{1}{\mathrm{i}\omega_{n_2}^{-}} f_{1100}^{1(3)} f_{1010}^{1(1)} + \frac{1}{-\mathrm{i}\omega_{n_1}^{+}} f_{1010}^{1(3)} f_{1100}^{1(1)} + \frac{1}{\mathrm{i}\omega_{n_2}^{-}} f_{1100}^{1(3)} f_{0110}^{1(2)} \\
& + 2\frac{1}{2\mathrm{i}\omega_{n_1}^{+}+\mathrm{i}\omega_{n_2}^{-}} f_{0200}^{1(3)} f_{1010}^{1(2)} + \frac{1}{\mathrm{i}\omega_{n_1}^{+}} f_{0110}^{1(3)} f_{1100}^{1(2)} + \frac{1}{-\mathrm{i}\omega_{n_1}^{+}} f_{1010}^{1(3)} f_{0110}^{1(3)} \\
& + \frac{1}{\mathrm{i}\omega_{n_1}^{+}} f_{0110}^{1(3)} f_{1010}^{1(3)} + \frac{2}{-\mathrm{i}\omega_{n_2}^{-}} f_{0020}^{1(3)} f_{1100}^{1(3)} + \frac{1}{-\mathrm{i}\omega_{n_1}^{+}+2\mathrm{i}\omega_{n_2}^{-}} f_{1001}^{1(3)} f_{0110}^{1(4)} \\
& + \frac{1}{\mathrm{i}\omega_{n_1}^{+}+2\mathrm{i}\omega_{n_2}^{-}} f_{0101}^{1(3)} f_{1010}^{1(4)} + \frac{1}{\mathrm{i}\omega_{n_2}^{-}} f_{0011}^{1(3)} f_{1100}^{1(4)}\Big), \\
E_{2100} = & \frac{1}{6\sqrt{l\pi}}\psi_1(0)[S_{yz_1}(w_{01100}) + S_{yz_2}(w_{02000})], \\
E_{1011} = & \frac{1}{6\sqrt{l\pi}}\psi_1(0)[S_{yz_1}(w_{00011}) + S_{yz_3}(w_{01001}) + S_{yz_4}(w_{01010})], \\
E_{0021} = & \frac{1}{6\sqrt{l\pi}}\psi_3(0)[S_{yz_3}(w_{00011}) + S_{yz_4}(w_{00020})], \\
E_{1110} = & \frac{1}{6\sqrt{l\pi}}\psi_3(0)[S_{yz_1}(w_{00110}) + S_{yz_2}(w_{01010}) + S_{yz_3}(w_{01100})],
\end{aligned}
$$

with

$$
\begin{aligned}
w_{02000}(\theta) = & \frac{1}{-\mathrm{i}\omega_{n_1}^{+}\tau^*}\phi_1(\theta) f_{2000}^{1(1)} + \frac{1}{-3\mathrm{i}\omega_{n_1}^{+}\tau^*}\phi_2(\theta) f_{2000}^{1(2)} + \frac{1}{-2\mathrm{i}\omega_{n_1}^{+}\tau^*+\mathrm{i}\omega_{n_2}^{-}\tau^*}\phi_3(\theta) f_{2000}^{1(3)} \\
& + \frac{1}{-2\mathrm{i}\omega_{n_1}^{+}\tau^*-\mathrm{i}\omega_{n_2}^{-}\tau^*}\phi_4(\theta) f_{2000}^{1(4)} - \frac{1}{\sqrt{l\pi}} e^{2\mathrm{i}\omega_{n_1}^{+}\tau^*\theta}[-2\mathrm{i}\omega_{n_1}^{+}\tau^* + L_0(e^{2\mathrm{i}\omega_{n_1}^{+}\tau^*}\cdot I)]^{-1} F_{2000}, \\
w_{01100}(\theta) = & \frac{1}{\mathrm{i}\omega_{n_1}^{+}\tau^*}\phi_1(\theta) f_{1100}^{1(1)} + \frac{1}{-\mathrm{i}\omega_{n_1}^{+}\tau^*}\phi_2(\theta) f_{1100}^{1(2)} + \frac{1}{\mathrm{i}\omega_{n_2}^{-}\tau^*}\phi_3(\theta) f_{1100}^{1(3)} \\
& + \frac{1}{-\mathrm{i}\omega_{n_2}^{-}\tau^*}\phi_4(\theta) f_{1100}^{1(4)} - \frac{1}{\sqrt{l\pi}}[L_0(I)]^{-1} F_{1100}, \\
w_{00011}(\theta) = & \frac{1}{\mathrm{i}\omega_{n_1}^{+}\tau^*}\phi_1(\theta) f_{0011}^{1(1)} + \frac{1}{-\mathrm{i}\omega_{n_1}^{+}\tau^*}\phi_2(\theta) f_{0011}^{1(2)} + \frac{1}{\mathrm{i}\omega_{n_2}^{-}\tau^*}\phi_3(\theta) f_{0011}^{1(3)} \\
& + \frac{1}{-\mathrm{i}\omega_{n_2}^{-}\tau^*}\phi_4(\theta) f_{0011}^{1(4)} - \frac{1}{\sqrt{l\pi}}[L_0(I)]^{-1} F_{0011}, \\
w_{01001}(\theta) = & \frac{1}{\mathrm{i}\omega_{n_2}^{-}\tau^*}\phi_1(\theta) f_{1001}^{1(1)} + \frac{1}{-2\mathrm{i}\omega_{n_1}^{+}\tau^*+\mathrm{i}\omega_{n_2}^{-}\tau^*}\phi_2(\theta) f_{1001}^{1(2)} \\
& + \frac{1}{-\mathrm{i}\omega_{n_1}^{+}\tau^*+2\mathrm{i}\omega_{n_2}^{-}\tau^*}\phi_3(\theta) f_{1001}^{1(3)} + \frac{1}{-\mathrm{i}\omega_{n_1}^{+}\tau^*}\phi_4(\theta) f_{1001}^{1(4)} \\
& - \frac{1}{\sqrt{l\pi}} e^{(\mathrm{i}\omega_{n_1}^{+}-\mathrm{i}\omega_{n_2}^{-})\tau^*\theta}[-(\mathrm{i}\omega_{n_1}^{+}-\mathrm{i}\omega_{n_2}^{-})\tau^* + L_0(e^{(\mathrm{i}\omega_{n_1}^{+}-\mathrm{i}\omega_{n_2}^{-})\tau^*}\cdot I)]^{-1} F_{1001}, \\
w_{01010}(\theta) = & \frac{1}{-\mathrm{i}\omega_{n_2}^{-}\tau^*}\phi_1(\theta) f_{1010}^{1(1)} + \frac{1}{-2\mathrm{i}\omega_{n_1}^{+}\tau^*-\mathrm{i}\omega_{n_2}^{-}\tau^*}\phi_2(\theta) f_{1010}^{1(2)} \\
& + \frac{1}{-\mathrm{i}\omega_{n_1}^{+}\tau^*}\phi_3(\theta) f_{1010}^{1(3)} + \frac{1}{-\mathrm{i}\omega_{n_1}^{+}\tau^*-2\mathrm{i}\omega_{n_2}^{-}\tau^*}\phi_4(\theta) f_{1010}^{1(4)}
\end{aligned}
$$

$$
\begin{aligned}
&- \frac{1}{\sqrt{l\pi}} e^{(\mathrm{i}\omega_{n_1}^{+}+\mathrm{i}\omega_{n_2}^{-})\tau^*\theta}[-(\mathrm{i}\omega_{n_1}^{+}+\mathrm{i}\omega_{n_2}^{-})\tau^* + L_0(e^{(\mathrm{i}\omega_{n_1}^{+}+\mathrm{i}\omega_{n_2}^{-})\tau^*}\cdot I)]^{-1}F_{1010},\\
w_{00110}(\theta) &= \frac{1}{2\mathrm{i}\omega_{n_1}^{+}\tau^* - \mathrm{i}\omega_{n_2}^{-}\tau^*}\phi_1(\theta)f_{0110}^{1(1)} + \frac{1}{-\mathrm{i}\omega_{n_2}^{-}\tau^*}\phi_2(\theta)f_{0110}^{1(2)}\\
&+ \frac{1}{\mathrm{i}\omega_{n_1}^{+}\tau^*}\phi_3(\theta)f_{0110}^{1(3)} + \frac{1}{\mathrm{i}\omega_{n_1}^{+}\tau^* - 2\mathrm{i}\omega_{n_2}^{-}\tau^*}\phi_4(\theta)f_{0110}^{1(4)}\\
&- \frac{1}{\sqrt{l\pi}} e^{(-\mathrm{i}\omega_{n_1}^{+}+\mathrm{i}\omega_{n_2}^{-})\tau^*\theta}[-(-\mathrm{i}\omega_{n_1}^{+}+\mathrm{i}\omega_{n_2}^{-})\tau^* + L_0(e^{(-\mathrm{i}\omega_{n_1}^{+}+\mathrm{i}\omega_{n_2}^{-})\tau^*}\cdot I)]^{-1}F_{0110},\\
w_{00020}(\theta) &= \frac{1}{\mathrm{i}\omega_{n_1}^{+}\tau^* - 2\mathrm{i}\omega_{n_2}^{-}\tau^*}\phi_1(\theta)f_{0020}^{1(1)} + \frac{1}{-\mathrm{i}\omega_{n_1}^{+}\tau^* - 2\mathrm{i}\omega_{n_2}^{-}\tau^*}\phi_2(\theta)f_{0020}^{1(2)} + \frac{1}{-\mathrm{i}\omega_{n_2}^{-}\tau^*}\phi_3(\theta)f_{0020}^{1(3)}\\
&+ \frac{1}{-3\mathrm{i}\omega_{n_2}^{-}\tau^*}\phi_4(\theta)f_{0020}^{1(4)} - \frac{1}{\sqrt{l\pi}} e^{2\mathrm{i}\omega_{n_2}^{-}\tau^*\theta}[-2\mathrm{i}\omega_{n_2}^{-}\tau^* + L_0(e^{2\mathrm{i}\omega_{n_2}^{-}\tau^*}\cdot I)]^{-1}F_{0020}.
\end{aligned}
$$

4. Numerical simulations

In this section, we carry out some numerical simulations to explain the theoretical results obtained in the previous sections. Symbolic mathematical software Matlab is used to plot numerical graphs. The delayed reaction-diffusion system (1.3) is numerically solved by transforming the continuous system to discrete system using discretization of time and space. In the discrete system, the Laplacian describing diffusion is calculated using finite differences, and the time evolution is solved using the Euler method. Fix the parameters as

$$
\begin{aligned}
&r_0 = 0.5,\ d = 0.1,\ a = 0.2,\ c = 0.9,\ m = 0.05,\ c_1 = 1,\\
&c_2 = 1,\ p = 0.9,\ q = 0.4,\ d_1 = 0.3,\ d_2 = 0.6,\ l = 8.
\end{aligned}
\tag{4.1}
$$

4.1. Three different cases induced by fear response delay τ

From Theorems 2, 3, 4, we have found that the fear response delay may have no effect, both stabilizing and destabilizing effect, or destabilizing effect on the stability of E^*, respectively. In this section, we explore that the impact level of fear k has on the stability of the positive equilibrium E^* and the occurrence of Hopf bifurcation induced by fear response delay.

Choose $k = 0.04$, such that the level of fear is low. We can verify that (H1) holds, thus $E^*(0.0659, 0.4483)$ exists. Moreover, (H2) and (H3) hold, which indicates that E^* is locally asymptotically stable for all $\tau > 0$ from Theorem 2. This indicates that the fear response delay does not change the stability of the positive equilibrium, which means that the fear response delay cannot support periodic oscillations in prey and predator populations with a low level of fear.

When k is increased to $k = 1$, the positive equilibrium $E^*(0.1299, 0.49)$ still exists, and (H1), (H2) and (H4) hold. By calculating the critical value of Hopf bifurcation in Table 1, we can get $\tau_0^{0+} < \tau_1^{0+} < \tau_1^{0-} < \tau_0^{0-} < \tau_0^{1+} < \tau_1^{1+} < \tau_0^{2+} < \tau_1^{2+}$. From Theorem 3, E^* is locally asymptotically stable when $\tau \in [0, \tau_0^{0+}) \cup (\tau_0^{0-}, \tau_0^{1+})$ (see Figures 1 and 3), and it is unstable when $\tau \in (\tau_0^{0+}, \tau_0^{0-}) \cup (\tau_0^{1+}, +\infty)$ (see Figures 2 and 4). It means that the fear response delay may lead to stability switches with an intermediate level of fear, which is not observed in the model with biomass transfer delay in [16].

When k is further increased to $k = 2.5$, we can verify that (H1), (H2) and (H7) hold, and we get $\tau_0^{0+} = 7.3868$. From Theorem 4, E^* is locally asymptotically stable when $\tau \in [0, \tau_0^{0+})$, and it is unstable

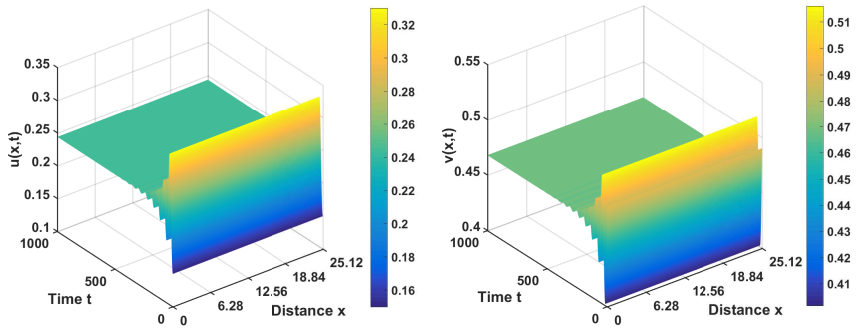

Figure 1. The positive equilibrium E^* is asymptotically stable when $\tau = 1 \in [0, \tau_0^{0+})$.

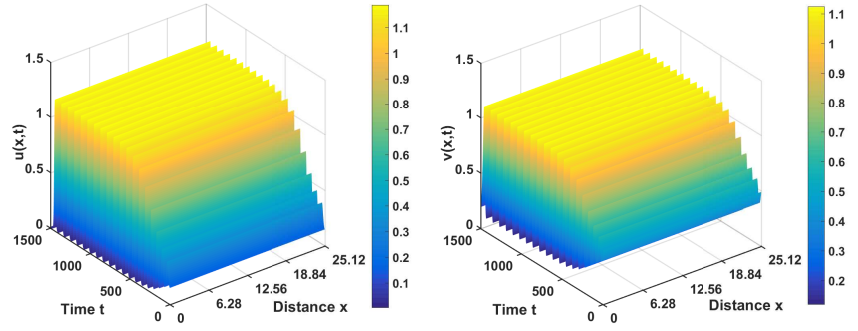

Figure 2. E^* is unstable and there is a bifurcating periodic solution when $\tau = 15 \in (\tau_0^{0+}, \tau_0^{0-})$.

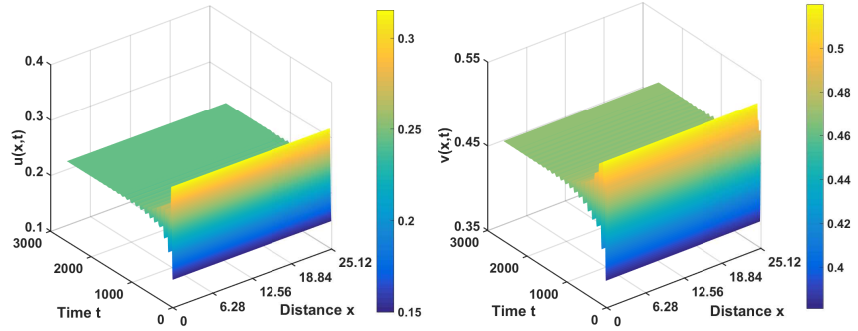

Figure 3. The positive equilibrium E^* is asymptotically stable when $\tau = 52 \in (\tau_0^{0-}, \tau_0^{1+})$.

Table 1. Critical values of Hopf bifurcation $\tau_n^{j\pm}$.

	$j=0$	$j=1$	$j=2$
$n=0$	$\tau_0^{0+}=3.048$	$\tau_0^{1+}=54.609$	$\tau_0^{2+}=106.169$
$n=0$	$\tau_0^{0-}=42.19$	$\tau_0^{1-}=132.59$	$\tau_0^{2-}=222.997$
$n=1$	$\tau_1^{0+}=6.203$	$\tau_1^{1+}=59.224$	$\tau_1^{2+}=112.244$
$n=1$	$\tau_1^{0-}=36.98$	$\tau_1^{1-}=122.64$	$\tau_1^{2-}=208.296$

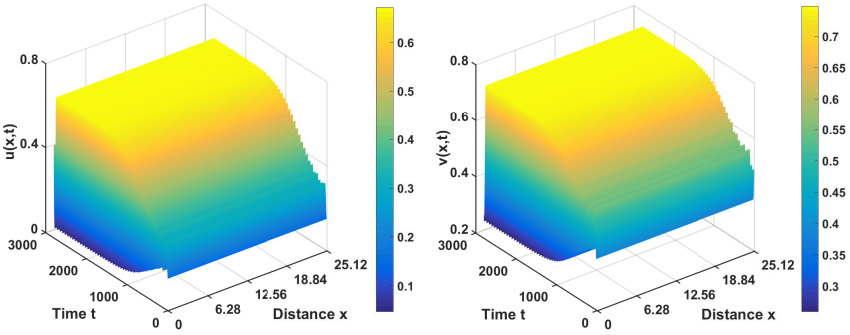

Figure 4. E^* is unstable and there is a bifurcating periodic solution when $\tau = 70 \in (\tau_0^{1+}, +\infty)$.

when $\tau > \tau_0^{0+}$.

4.2. The joint effect of k and τ

In this section, we explore the joint effect of the fear level and fear response delay on the dynamics of system (1.3). We choose k and τ as bifurcation parameters, and other parameters are the same as in (4.1). From (2.12), we can draw Hopf bifurcation curves with varying k (see Figure 5). Hopf bifurcation curve τ_0^{1+} intersects with τ_0^{0-} at HH $(k^*, \tau^*) = (1.3677, 58.6677)$. On HH, Eq (2.6) has two pairs of purely imaginary roots $\pm i\omega_0^- = \pm 0.0503$ i, $\pm i\omega_0^+ = \pm 0.1146$ i. Therefore, HH is a possible double Hopf bifurcation point. By the calculation of normal form of double Hopf bifurcation, we can

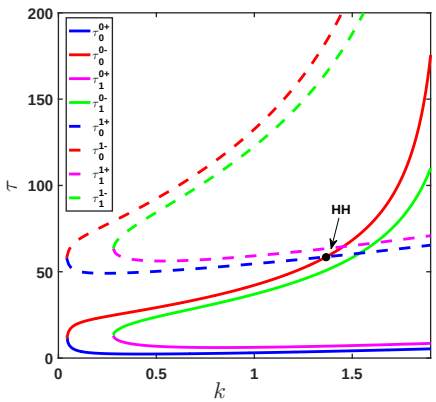

Figure 5. The bifurcation diagram on (k, τ) plane.

get the coefficients in (3.5) with

$$\begin{aligned} &B_{11} \approx 0.6682 - 0.4239\,\mathrm{i}, \quad B_{21} \approx -0.0108 + 0.0082\,\mathrm{i},\\ &B_{13} \approx -0.4482 - 0.2903\,\mathrm{i}, \quad B_{23} \approx 0.03817 + 0.0424\,\mathrm{i},\\ &B_{2100} \approx 0.3385 - 2.1955\,\mathrm{i}, \quad B_{1011} \approx 0.5068 + 0.6607\,\mathrm{i},\\ &B_{0021} \approx -0.7364 - 0.774\,\mathrm{i}, \quad B_{1110} \approx -4.2835 + 2.426\,\mathrm{i}. \end{aligned}$$

Make the polar coordinate transformation

$$\begin{aligned} &z_1 = r_1\cos\theta_1 + \mathrm{i}r_1\sin\theta_1, \quad z_2 = r_1\cos\theta_1 - \mathrm{i}r_1\sin\theta_1,\\ &z_3 = r_2\cos\theta_2 + \mathrm{i}r_2\sin\theta_2, \quad z_4 = r_2\cos\theta_2 - \mathrm{i}r_2\sin\theta_2, \end{aligned}$$

and denote

$$\epsilon_1 = \mathrm{Sign}(\mathrm{Re}B_{2100}),\ \epsilon_2 = \mathrm{Sign}(\mathrm{Re}B_{0021}),\ \bar{r}_1 = r_1\sqrt{|B_{2100}|},\ \bar{r}_2 = r_2\sqrt{|B_{0021}|},\ \bar{t} = t\varepsilon_1.$$

Removing the bars, the four-dimensional system (3.5) is transformed into the following two-dimensional amplitude system

$$\begin{aligned} \dot{r}_1 &= r_1(0.6682\,\alpha_1 - 0.0108\,\alpha_2 + r_1^2 + 0.6885\,r_2^2),\\ \dot{r}_2 &= r_2(-0.4482\,\alpha_1 + 0.0382\,\alpha_2 - 12.6574\,r_1^2 - r_2^2). \end{aligned} \tag{4.2}$$

By a simple calculation, we find that the system (4.2) admits the following equilibria

$$\begin{aligned} &A_0 = (0,0),\\ &A_1 = (\sqrt{0.0108\alpha_2 - 0.6682\alpha_1}, 0),\ \text{for}\ \alpha_1 < 0.0162\alpha_2,\\ &A_2 = (0, \sqrt{0.0382\alpha_2 - 0.4482\alpha_1}),\ \text{for}\ \alpha_1 < 0.0852\alpha_2,\\ &A_3 = (\sqrt{0.0466\alpha_1 + 0.002\alpha_2}, \sqrt{-1.0382\alpha_1 + 0.0128\alpha_2}),\ \text{for}\ -0.0429\alpha_2 < \alpha_1 < 0.0123\alpha_2. \end{aligned}$$

According to [29], the unfolding of system (4.2) is of type VIa. There are rays $L_1 - L_8$ near the bifurcation point, which divide the phase space into eight parts (see Figure 6(a)), where

$$\begin{aligned} &L_1 : \tau = \tau^* + 11.7406\,(k-k^*)\ \ (k>k^*); && L_2 : \tau = \tau^* + 61.7604\,(k-k^*)\ \ (k>k^*);\\ &L_3 : \tau = \tau^* + 81.0926\,(k-k^*)\ \ (k>k^*); && L_4 : \tau = \tau^* + 100.462\,(k-k^*) + o(k-k^*)\ \ (k>k^*);\\ &L_5 : \tau = \tau^* + 100.462\,(k-k^*)\ \ (k>k^*); && L_6 : \tau = \tau^* - 23.3449\,(k-k^*)\ \ (k<k^*);\\ &L_7 : \tau = \tau^* + 11.7406\,(k-k^*)\ \ (k<k^*); && L_8 : \tau = \tau^* + 61.7604\,(k-k^*)\ \ (k<k^*). \end{aligned}$$

The detailed dynamics in $D_1 - D_8$ near (k^*, τ^*) have shown in Figure 6(b).

Notice that A_0 of (4.2) corresponds to the positive equilibrium E^* of the original system (1.3). A_1 and A_2 correspond to the periodic solution of (1.3). A_3 corresponds to quasi-periodic solution on a 2-torus. Periodic orbit of (4.2) corresponds to quasi-periodic solution on a 3-torus. Due to the fact that double Hopf bifurcation point HH is the intersection of 0-mode Hopf bifurcation curves τ_0^{1+} and τ_0^{0-}, all periodic or quasi-periodic solutions near HH are spatially homogeneous.

In region D_1, system (4.2) has only one equilibrium A_0, which is a saddle. It means that the positive equilibrium $E^*(u^*, v^*)$ of system (1.3) is unstable.

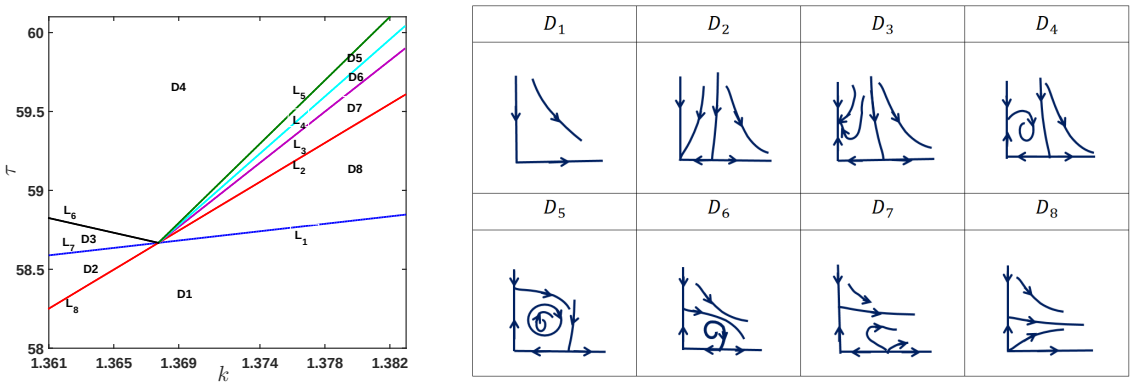

(a) (b)

Figure 6. (a) The bifurcation diagram on (k, τ) plane. (b) The complete bifurcation set around HH.

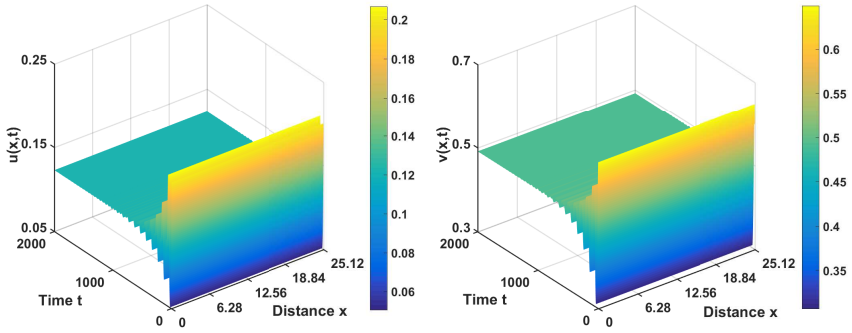

Figure 7. When $k = 0.9, \tau = 50$ in D_2, the positive equilibrium $E^*(u^*, v^*)$ is asymptotically stable.

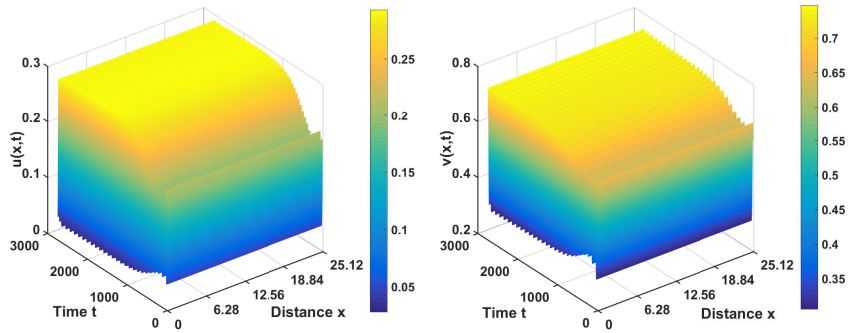

Figure 8. When $k = 0.8, \tau = 55$ in D_3, the periodic solutions are stable.

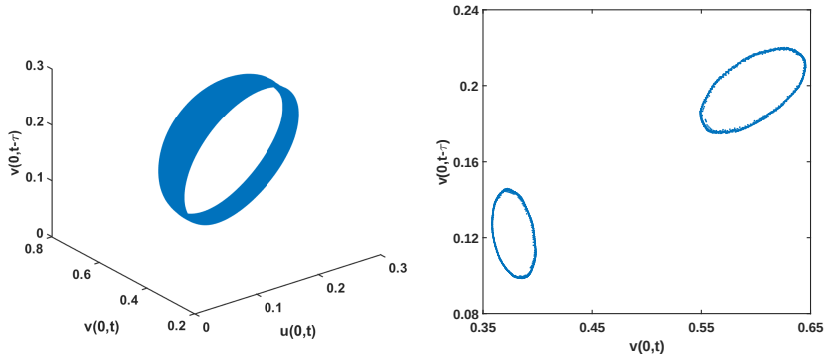

Figure 9. There is a stable quasi-periodic solution on a 2-torus of system (1.3) when $(k, \tau) = (1.345, 59.5) \in D_4$.

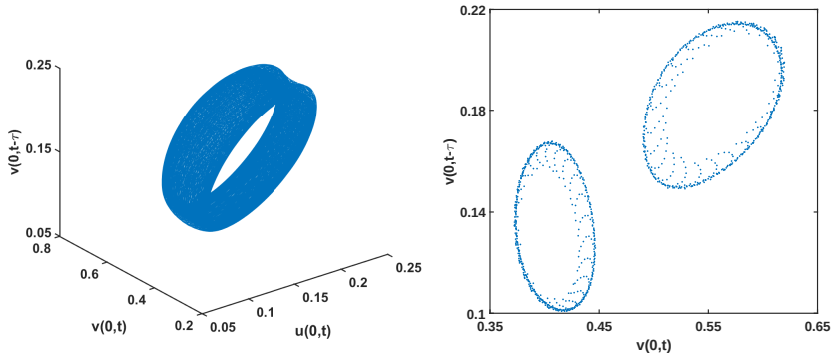

Figure 10. There is a stable quasi-periodic solution on a 3-torus of system (1.3) when $(k, \tau) = (1.364, 59.4) \in D_5$.

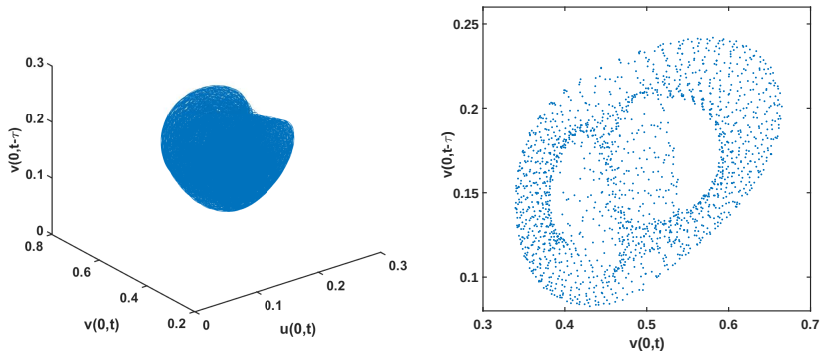

Figure 11. When $(k, \tau) = (1.3801, 59.978) \in D_6$, the system has chaotic behavior and there is a strange attractor of system (1.3).

In region D_2, the trivial equilibrium A_0 of (4.2) is a sink, and A_1 is unstable. This means that $E^*(u^*, v^*)$ of system (1.3) is asymptotically stable as shown in Figure 7, when $k = 0.9$ and $\tau = 50$ are chosen in D_2. In addition, the spatially homogeneous periodic solution is born, which is unstable.

In region D_3, system (4.2) has three equilibria: A_0, A_1 and A_2. A_2 is stable while other equilibria are unstable. When $k = 0.8$ and $\tau = 55$ are chosen in D_3, system (1.3) has spatially homogeneous periodic solution, which is stable (see Figure 8).

In region D_4, there are four equilibria of (4.2): A_0, A_1, A_2 and A_3. A_3 is stable while other equilibria are unstable. Since the double Hopf bifurcation occurs at the intersection of two Hopf bifurcation curves with $n = 0$, we choose $x = 0$ to demonstrate the rich dynamical phenomena of system (1.3). When parameters are chosen as $k = 1.345$ and $\tau = 59.5$ in D_4, system (1.3) has a quasi-periodic solution on 2-torus, which is shown in Figure 9.

In region D_5, there are four equilibria and a periodic orbit of (4.2). A_0, A_1, A_2 and A_3 are all unstable, and the periodic orbit is stable. This means that system (1.3) has a stable quasi-periodic solution on a 3-torus. Figure 10 illustrates the existence of a stable quasi-periodic solution on a 3-torus when $k = 1.364$ and $\tau = 59.4$ are chosen in D_5.

In region D_6, system (4.2) has four equilibria: A_0, A_1, A_2 and A_3, which are all unstable. When the parameter enters region D_6, the 3-torus disappears through heteroclinic orbits, and the system (1.3) generates strange attractor according to the "the Ruelle-Takens-Newhouse" scenario. Figure 11 illustrates system (1.3), which demonstrates chaotic phenomena when $k = 1.3801$ and $\tau = 59.978$ are chosen in D_6. The right figures of Figure 9, 10 and 11 are the results of Poincaré map on a Poincaré section.

In region D_7, system (4.2) has three equilibria: A_0, A_1 and A_2, which are all unstable. This means that the positive equilibrium $E^*(u^*, v^*)$ and the spatially homogeneous periodic solutions of system (1.3) are all unstable.

In region D_8, system (4.2) has two equilibria: A_0 and A_2, which are both unstable. This means that the positive equilibrium $E^*(u^*, v^*)$ and the spatially homogeneous periodic solution of system (1.3) are all unstable.

5. Conclusion and future work

There have been more and more evidences showing that fear from the predator may affect the behavior and physiology of prey, which could reduce the reproduction of prey [1, 6, 7]. Moreover, anti-predation behavior of scared prey can also reduce the chance of prey being caught by predators. Therefore, we consider a predator-prey model with both costs and benefits due to fear based on [16]. Since the cost of fear in prey reproduction is not instantaneous, we incorporate a fear response delay into the model. Our aim is to explore how the fear level and fear response delay jointly affect the dynamics of the predator-prey system from the point of view of both codimension-1 and codimension-2 bifurcation analysis.

First, we find that Turing instability does not occur in our model. Since the pioneering work of Turing [30], quite a number of literature has revealed that diffusion might destabilize an equilibrium and generate spatial pattern formation. However, not all diffusive systems exhibit such diffusion-driven instability. In some chemical and biological models, Turing instability induced by diffusion are not observed [31–33].

Next, we explore the role of fear response delay on the dynamics. Through the analysis of the characteristic equation, it turns out that there are three different cases: the fear response delay may have no effect, both stabilizing and destabilizing effect, or destabilizing effect on the stability of E^*, which are shown in Theorems 2, 3, 4, respectively. Combining with numerical simulations, it is found that the the occurrence of Hopf bifurcation induced by fear response delay has closely connection with the fear level. When the fear level is low, the delay could not change the stability of the positive equilibrium, which is asymptotically stable for all τ. From the point of view of biology, the fear response delay cannot support periodic oscillations in prey and predator populations with a low level of fear. When the fear level is in an intermediate range, the fear response delay can induce stability switches, which indicates that the delay has effects on both destabilizing and stabilizing the dynamics. It is observed that such stability switches cannot be generated by the biomass transfer delay [16]. When the fear level is high, the fear response delay can destabilize the equilibrium and induce Hopf bifurcation.

Finally, to better reveal the joint effect of fear level and fear response delay on the dynamics of system (1.3), we carry out codimension-2 bifurcation analysis. On the (k, τ) plane, by finding the interactions of Hopf bifurcation curves, we can find the possible critical point of double Hopf bifurcation. After the calculation of the normal form for double Hopf bifurcation, we can obtain the bifurcation set, and figure out all the dynamical behaviors around the critical point. There are periodic solutions, quasi-periodic solutions and even chaos observed near the double Hopf bifurcation point.

In this paper, we assume that the interaction between individuals of a species is local. The individuals at different locations may compete for common resource or communicate visually or by chemical means. Regarding fear effect, the fear of predator depends on both the local and nearby appearance of the predator. Taking these into account, the influence of the nonlocal effect on the spatiotemporal dynamics of the diffusive predator-prey model with fear would be worth further study. In addition, we consider diffusion induced by random movement, however, cognition and memory also have an important influence on the animal movement. Shi et al. [34] proposed a memory-based diffusion equation of a single species. Memory-based diffusion can be modified and applied to the model with fear effect, which will provide much more realistic results and bring mathematical challenges.

Use of AI tools declaration

The authors declare they have not used Artificial Intelligence (AI) tools in the creation of this article.

Acknowledgments

The work is supported by National Natural Science Foundation of China (Nos. 11901369, 11971281 and 12071268) and PhD research startup foundation of Shaanxi University of Science and Technology (2023BJ-13).

Conflict of interest

The authors declare there is no conflicts of interest.

References

1. É. Diz-Pita, M. V. Otero-Espinar, Predator–prey models: A review of some recent advances, *Mathematics*, **9** (2021), 1783. https:// https://doi.org/10.3390/math9151783
2. Q. J. A. Khan, E. Balakrishnan, G. C. Wake, Analysis of a predator-prey system with predator switching, *B. Math. Biol.*, **66** (2004), 109–123. https://doi.org/10.1016/j.bulm.2003.08.005
3. S. Liu, E. Beretta, A stage-structured predator-prey model of Beddington-DeAngelis type, *Siam. J. Appl. Math.*, **66** (2006), 1101–1129. https://doi.org/10.1137/050630003
4. J. M. Jeschke, M. Kopp, R. Tollrian, Predator functional responses: Discriminating between handling and digesting prey, *Ecol. Monogr.*, **72** (2002), 95–112. https://doi.org/10.1890/0012-9615(2002)072[0095:PFRDBH]2.0.CO;2
5. C. S. Holling, The functional response of predators to prey density and its role in mimicry and population regulation, *Mem. Entomol. Soc. Can.*, **97** (1965), 5–60. https://doi.org/10.4039/entm9745fv
6. L. Y. Zanette, A. F. White, M. C. Allen, M. Clinchy, Perceived predation risk reduces the number of offspring songbirds produce per year, *Science*, **334** (2011), 1398–140. https://doi.org/10.1126/science.1210908
7. W. Cresswell, Predation in bird populations, *J. Ornithol.*, **152** (2011), 251–263. https://doi.org/10.1007/s10336-010-0638-1
8. X. Wang, L. Zanette, X. Zou, Modelling the fear effect in predator-prey interactions, *J. Math. Biol.*, **73** (2016), 1179–1204. https://doi.org/10.1007/s00285-016-0989-1
9. Y. Shi, J. Wu, Q. Cao, Analysis on a diffusive multiple Allee effects predator-prey model induced by fear factors, *Nonlinear Anal. Real*, **59** (2021), 103249. https://doi.org/10.1016/j.nonrwa.2020.103249
10. X. Zhang, H. Zhao, Y. Yuan, Impact of discontinuous harvesting on a diffusive predator-prey model with fear and Allee effect, *Z. Angew. Math. Phys.*, **73** (2022), 1–29. https://doi.org/10.1007/s00033-022-01807-8
11. S. Pal, N. Pal, S. Samanta, J. Chattopadhyay, Fear effect in prey and hunting cooperation among predators in a Leslie-Gower model, *Math. Biosci. Eng.*, **16** (2019), 5146–5179. https://doi.org/10.3934/mbe.2019258
12. P. Panday, N. Pal, S. Samanta, P. Tryjanowski, Dynamics of a stage-structured predator-prey model: cost and benefit of fear-induced group defense, *J. Theor. Biol.*, **528** (2021), 110846. https://doi.org/10.1016/j.jtbi.2021.110846
13. S. K. Sasmal, Y. Takeuchi, Dynamics of a predator-prey system with fear and group defense, *J. Math. Anal. Appl.*, **481** (2020), 123471. https://doi.org/10.1016/j.jmaa.2019.123471
14. N. Zhang, Y. Kao, B. Xie, Impact of fear effect and prey refuge on a fractional order prey-predator system with Beddington-DeAngelis functional response, *Chaos*, **32** (2022), 043125. https://doi.org/10.1063/5.0082733
15. H. Chen, C. Zhang, Dynamic analysis of a Leslie-Gower-type predator-prey system with the fear effect and ratio-dependent Holling III functional response, *Nonlinear Anal-Model.*, **27** (2022), 904–926. https://doi.org/10.15388/namc.2022.27.27932

16. Y. Wang, X. Zou, On a predator-prey system with digestion delay and anti-predation strategy, *J. Nonlinear Sci.*, **30** (2020), 1579–1605. https://doi.org/10.1007/s00332-020-09618-9

17. B. Dai, G. Sun, Turing-Hopf bifurcation of a delayed diffusive predator-prey system with chemotaxis and fear effect, *Appl. Math. Lett.*, **111** (2021), 106644. https://doi.org/10.1016/j.aml.2020.106644

18. X. Zhang, Q. An, L. Wang, Spatiotemporal dynamics of a delayed diffusive ratio-dependent predator-prey model with fear effect, *Nonlinear Dyn.*, **105** (2021), 3775–3790. https://doi.org/10.1007/s11071-021-06780-x

19. C. Wang, S. Yuan, H. Wang, Spatiotemporal patterns of a diffusive prey-predator model with spatial memory and pregnancy period in an intimidatory environment, *J. Math. Biol.*, **84** (2022), 12. https://doi.org/10.1007/s00285-022-01716-4

20. J. Liu, Y. Kang, Spatiotemporal dynamics of a diffusive predator-prey model with fear effect, *Nonlinear Anal-Model.*, **27** (2022), 841–862. https://doi.org/10.15388/namc.2022.27.27535

21. X. Wang, X. Zou, Pattern formation of a predator-prey model with the cost of anti-predator behaviors, *Math. Biosci. Eng.*, **15** (2018), 775–805. https://doi.org/10.3934/mbe.2018035

22. J. P. Tripathi, S. Bugalia, D. Jana, N. Gupta, V. Tiwari, J. Li, et al., Modeling the cost of anti-predator strategy in a predator-prey system: The roles of indirect effect, *Math. Methods Appl. Sci.*, **45** (2022), 4365-4396. https://doi.org/10.1002/mma.8044

23. D. Duan, B. Niu, J. Wei, Hopf-Hopf bifurcation and chaotic attractors in a delayed diffusive predator-prey model with fear effect, *Chaos Solitons Fractals*, **123** (2019), 206–216. https://doi.org/10.1016/j.chaos.2019.04.012

24. P. Panday, S. Samanta, N. Pal, J. Chattopadhyay, Delay induced multiple stability switch and chaos in a predator-prey model with fear effect, *Math. Comput. Simul.*, **172** (2020), 134–158. https://doi.org/10.1016/j.matcom.2019.12.015

25. B. Dubey, A. Kumar, Stability switching and chaos in a multiple delayed prey-predator model with fear effect and anti-predator behavior, *Math. Comput. Simulat.*, **188** (2021), 164–192. https://doi.org/10.1016/j.matcom.2021.03.037

26. Y. Song, Q. Shi, Stability and bifurcation analysis in a diffusive predator-prey model with delay and spatial average, *Math. Method. Appl. Sci.*, **5** (2023), 5561–5584. https://doi.org/10.1002/mma.8853

27. D. Geng, W. Jiang, Y. Lou, H. Wang, Spatiotemporal patterns in a diffusive predator-prey system with nonlocal intraspecific prey competition, *Stud. Appl. Math.*, **148** (2022), 396–432. https://doi.org/10.1111/sapm.12444

28. Y. Du, B. Niu, Y. Guo, J. Wei, Double Hopf bifurcation in delayed reaction-diffusion systems, *J. Dyn. Differ. Equ.*, **32** (2020), 313–358. https://doi.org/10.1007/s10884-018-9725-4

29. J. Guckenheimer, P. Holmes, Local codimension two bifurcations of flows in *Nonlinear Oscillations, Dynamical Systems, and Bifurcations of Vector Fields*, Springer, (1983), 397–411. https://doi.org/10.1007/978-1-4612-1140-2

30. A. M. Turing, The chemical basis of morphogenesis, *B. Math. Biol.*, **52** (1990), 153–197. https://doi.org/10.1016/S0092-8240(05)80008-4

31. Y. Almirantis, S. Papageorgiou, Cross-diffusion effects on chemical and biological pattern formation, *J. Theor. Biol.*, **151** (1991), 289–311. https://doi.org/10.1016/S0022-5193(05)80379-0

32. J. Chattopadhyay, P. K. Tapaswi, Effect of cross-diffusion on pattern formation-a nonlinear analysis, *Acta Appl. Math.*, **48** (1997), 1–12. https://doi.org/10.1023/A:1005764514684

33. J. Zhao, J. Wei, Dynamics in a diffusive plankton system with delay and toxic substances effect, *Nonlinear Anal. Real*, **22** (2015), 66–83. https://doi.org/10.1016/j.nonrwa.2014.07.010

34. J. Shi, C. Wang, H. Wang, X. Yan, Diffusive spatial movement with memory, *J. Dyn. Differ.*, **32** (2020), 979–1002. https://doi.org/10.1007/s10884-019-09757-y

Appendix A: The proof of Lemma 5

By direct calculation, we have

$$\begin{aligned}\frac{\mathrm{d}[(\omega_n^+)^2 - D_n]}{\mathrm{d}n} &= 2\omega_n^+ \cdot \frac{\mathrm{d}\omega_n^+}{\mathrm{d}n} - \frac{\mathrm{d}D_n}{\mathrm{d}n} \\ &= \frac{1}{2}\left\{-\frac{\mathrm{d}(T_n^2 - 2D_n)}{\mathrm{d}n} + \frac{1}{\sqrt{\Delta}} \cdot \left[(T_n^2 - 2D_n) \cdot \frac{\mathrm{d}(T_n^2 - 2D_n)}{\mathrm{d}n} - 2\frac{\mathrm{d}(D_n^2 - M^2)}{\mathrm{d}n}\right]\right\} - \frac{\mathrm{d}D_n}{\mathrm{d}n}.\end{aligned}$$

From Lemma 1, we have $\frac{\mathrm{d}(T_n^2-2D_n)}{\mathrm{d}n} > 0$, $\frac{\mathrm{d}(D_n^2-M^2)}{\mathrm{d}n} > 0$. Moreover, from (2.10), we know that $T_n^2 - 2D_n < 0$ for $0 \le n \le n_1$. Combining $\frac{\mathrm{d}D_n}{\mathrm{d}n} > 0$ and $M > 0$, we have $\frac{\mathrm{d}[(\omega_n^+)^2-D_n]}{\mathrm{d}n} < 0$, and $\frac{\mathrm{d}[\arccos(\frac{(\omega_n^+)^2-D_n}{M})+2j\pi]}{\mathrm{d}n} > 0$. Similarly, we can also prove that $\frac{\mathrm{d}\omega_n^+}{\mathrm{d}n} < 0$. Thus, τ_n^{j+} is monotonically increasing with respect to n.

Now we consider the monotonicity for τ_n^{j-}.

$$\begin{aligned}\frac{\mathrm{d}[(\omega_n^-)^2 - D_n]}{\mathrm{d}n} &= \frac{1}{2}\left\{-\frac{\mathrm{d}(T_n^2 - 2D_n)}{\mathrm{d}n} - \frac{1}{\sqrt{\Delta}} \cdot \left[(T_n^2 - 2D_n) \cdot \frac{\mathrm{d}(T_n^2 - 2D_n)}{\mathrm{d}n} - 2\frac{\mathrm{d}(D_n^2 - M^2)}{\mathrm{d}n}\right]\right\} - \frac{\mathrm{d}D_n}{\mathrm{d}n} \\ &= -\frac{1}{2} \cdot \frac{\mathrm{d}(T_n^2 - 2D_n)}{\mathrm{d}n} \cdot \left[\frac{\sqrt{\Delta} + (T_n^2 - 2D_n)}{\sqrt{\Delta}}\right] + \frac{1}{\sqrt{\Delta}} \cdot \frac{\mathrm{d}(D_n^2 - M^2)}{\mathrm{d}n} - \frac{\mathrm{d}D_n}{\mathrm{d}n}.\end{aligned}$$

Since $D_n^2 - M^2 > 0$ for all $n \in \mathbb{N}_0$, and $T_n^2 - 2D_n < 0$ for $0 \le n \le n_1$, then $\sqrt{\Delta} + T_n^2 - 2D_n < 0$ for $0 \le n \le n_1$. Combining with Lemma 1, we have $-\frac{\mathrm{d}(T_n^2-2D_n)}{\mathrm{d}n} \cdot \left[\frac{\sqrt{\Delta}+(T_n^2-2D_n)}{\sqrt{\Delta}}\right] > 0$. From $T_n^2 - 2D_n < 0$, and $D_n^2 > M^2$, we have $4D_n^2 - \Delta = 4(D_n^2 - M^2) + T_n^2(4D_n - T_n^2) > 0$, and thus $2D_n - \sqrt{\Delta} > 0$. From $\frac{\mathrm{d}D_n}{\mathrm{d}n} > 0$, we get $\frac{1}{\sqrt{\Delta}} \cdot \frac{\mathrm{d}(D_n^2-M^2)}{\mathrm{d}n} - \frac{\mathrm{d}D_n}{\mathrm{d}n} = \frac{\mathrm{d}D_n}{\mathrm{d}n} \cdot \left[\frac{2D_n-\sqrt{\Delta}}{\sqrt{\Delta}}\right] > 0$. Therefore, $\frac{\mathrm{d}[(\omega_n^-)^2-D_n]}{\mathrm{d}n} > 0$, and $\frac{\mathrm{d}[\arccos(\frac{(\omega_n^-)^2-D_n}{M})+2j\pi]}{\mathrm{d}n} < 0$. $\frac{\mathrm{d}[(\omega_n^-)^2-D_n]}{\mathrm{d}n} > 0$ can also lead to $\frac{\mathrm{d}\omega_n^-}{\mathrm{d}n} > 0$. Thus, τ_n^{j-} is monotonically decreasing with respect to n.

Appendix B: The coefficients of nonlinear terms

$$
\begin{aligned}
F_{uu} &= 2\tau^*\left(-a + \frac{pqv^*}{(1+qu^*)^3(1+c_1k)}, -\frac{pqcv^*}{(1+qu^*)^3(1+c_1k)}\right)^T,\\
F_{uv} &= \tau^*\left(-\frac{p}{(1+qu^*)^2(1+c_1k)}, \frac{cp}{(1+qu^*)^2(1+c_1k)}\right)^T,\\
F_{uv_t} &= \tau^*\left(-\frac{r_0c_2k}{(1+c_2kv^*)^2}, 0\right)^T, \quad F_{v_tv_t} = 2\tau^*\left(\frac{r_0u^*c_2^2k^2}{(1+c_2kv^*)^3}, 0\right)^T,\\
F_{uuu} &= 6\tau^*\left(-\frac{pq^2v}{(1+qu^*)^4(1+c_1k)}, \frac{pq^2cv^*}{(1+qu^*)^4(1+c_1k)}\right)^T,\\
F_{uuv} &= 2\tau^*\left(\frac{pq}{(1+qu^*)^3(1+c_1k)}, -\frac{pqc}{(1+qu^*)^3(1+c_1k)}\right)^T,\\
F_{uv_tv_t} &= 2\tau^*\left(\frac{r_0c_2^2k^2}{(1+c_2kv^*)^3}, 0\right)^T, \quad F_{v_tv_tv_t} = 6\tau^*\left(-\frac{r_0u^*c_2^3k^3}{(1+c_2kv^*)^4}, 0\right)^T.
\end{aligned}
$$

Appendix C: Some terms in $F_2(\alpha_1, \alpha_2, U_t)$

From the expression of $F_2(\alpha_1, \alpha_2, U_t)$,

$$
\begin{aligned}
L_1^{(1,0)}U_t &= \tau^*[G_0(k^*+\alpha_1)U_t(0) + G_1(k^*+\alpha_1)U_t(-1)] - L_0U_t\\
&= \tau^*[G_0'(k^*)U_t(0) + G_1'(k^*)U_t(-1)],
\end{aligned}
$$

where

$$
\begin{aligned}
J_{11}'(k^*) &= \frac{pq[u^{*'}(k^*)v^*(k^*) + u^*(k^*)v^{*'}(k^*)]xy - pqu^*(k^*)v^*(k^*)h}{x^2y^3} - au^{*'}(k^*),\\
J_{12}'(k^*) &= -\frac{pu^{*'}(k^*)xy - pu^*(k^*)[c_1y + qu^{*'}(k^*)x]}{x^2y^2},\\
J_{21}'(k^*) &= \frac{cpv^{*'}(k^*)}{xy^2} - \frac{cpv^*(k^*)h}{x^2y^3},\\
K_{12}'(k^*) &= -\frac{r_0c_2[u^*(k^*) + k^*u^{*'}(k^*)]z - 2r_0k^*c_2^2u^*(k^*)[v^*(k^*) + k^*v^{*'}(k^*)]}{z^3},
\end{aligned}
$$

with $x = 1 + c_1k^*$, $y = 1 + qu^*(k^*)$, $z = 1 + c_2k^*v^*(k^*)$, $h = c_1y + 2qu^{*'}(k^*)x$,

$$a_0'(k^*) = c_2 p,\ \ a_1'(k^*) = ac_1 k^* u^{*'}(k^*)xy + (d + au^*(k^*))[qc_1 k^* u^{*'}(k^*)x + yc_1(c_1 k^* + x)],$$
$$a_2'(k^*) = au^{*'}(k^*)xy + [d + au^*(k^*) - r_0][qu^{*'}(k^*)x + c_1 y],$$
$$u^{*'}(k^*) = \frac{cc_1 mp}{[cp - mq(1 + c_1 k^*)]^2},$$
$$v^{*'}(k^*) = \frac{-a_1'(k^*) + [a_1^2(k^*) - 4a_0(k^*)a_2(k^*)]^{-\frac{1}{2}}[a_1(k^*)a_1'(k^*) - 2(a_0'(k^*)a_2(k^*) + a_0(k^*)a_2'(k^*))]}{2a_0(k^*)}$$
$$+ \frac{a_0'(k^*)[a_1(k^*) - (a_1^2(k^*) - 4a_0(k^*)a_2(k^*))^{\frac{1}{2}}]}{2a_0^2(k^*)}.$$

Appendix D: $\widetilde{F}_2(z, y, \alpha)$ and $\widetilde{F}_3(z, 0, 0)$

$$\widetilde{F}_2(z, y, \alpha) = \sum_{q_1+q_2+q_3+q_4=2} F_{q_1q_2q_3q_4}\gamma_{n_1}^{q_1+q_2}(x)\gamma_{n_2}^{q_3+q_4}(x)z_1^{q_1}z_2^{q_2}z_3^{q_3}z_4^{q_4}$$
$$+ S_{yz_1}(y)z_1\gamma_{n_1} + S_{yz_2}(y)z_2\gamma_{n_1} + S_{yz_3}(y)z_3\gamma_{n_2} + S_{yz_4}(y)z_4\gamma_{n_2} + o(z^2, y^2),$$
$$\widetilde{F}_3(z, 0, 0) = \sum_{q_1+q_2+q_3+q_4=3} F_{q_1q_2q_3q_4}\gamma_{n_1}^{q_1+q_2}(x)\gamma_{n_2}^{q_3+q_4}(x)z_1^{q_1}z_2^{q_2}z_3^{q_3}z_4^{q_4},$$

Here $S_{yz_i}(i = 1, 2, 3, 4)$ are linear operators and

$$S_{yz_i}(y) = (F_{y_1(0)z_i}, F_{y_2(0)z_i})y(0) + (F_{y_1(-1)z_i}, F_{y_2(-1)z_i})y(-1),$$

where

$$F_{y_1(0)z_1} = 2(F_{uu} + p_{12}F_{uv} + p_{12}e^{-i\omega_{n_1}^+\tau^*}F_{uv_t}), \quad F_{y_2(0)z_1} = 2F_{uv},$$
$$F_{y_1(-1)z_1} = 0, \quad F_{y_2(-1)z_1} = 2(F_{uv_t} + p_{12}e^{-i\omega_{n_1}^+\tau^*}F_{v_tv_t}),$$
$$F_{y_1(0)z_3} = 2(F_{uu} + p_{32}F_{uv} + p_{32}e^{-i\omega_{n_2}^-\tau^*}F_{uv_t}), \quad F_{y_2(0)z_3} = 2F_{uv},$$
$$F_{y_1(-1)z_3} = 0, \quad F_{y_2(-1)z_3} = \overline{2(F_{uv_t} + p_{32}e^{-i\omega_{n_2}^-\tau^*}F_{v_tv_t})},$$
$$F_{y_1(0)z_2} = \overline{F_{y_1(0)z_1}}, \quad F_{y_2(0)z_2} = \overline{F_{y_2(0)z_1}},$$
$$F_{y_1(-1)z_2} = \overline{F_{y_1(-1)z_1}}, \quad F_{y_2(-1)z_2} = \overline{F_{y_2(-1)z_1}},$$
$$F_{y_1(0)z_4} = \overline{F_{y_1(0)z_3}}, \quad F_{y_2(0)z_4} = \overline{F_{y_2(0)z_3}},$$
$$F_{y_1(-1)z_4} = \overline{F_{y_1(-1)z_3}}, \quad F_{y_2(-1)z_4} = \overline{F_{y_2(-1)z_3}},$$

and

$$
\begin{aligned}
F_{2000} &= F_{uu} + 2p_{12}F_{uv} + 2p_{12}e^{-\mathrm{i}\omega_{n_1}^{+}\tau^{*}}F_{uv_t} + p_{12}^{2}e^{-2\mathrm{i}\omega_{n_1}^{+}\tau^{*}}F_{v_tv_t},\\
F_{1100} &= 2(F_{uu} + (p_{12} + \bar{p}_{12})F_{uv} + (p_{12}e^{-\mathrm{i}\omega_{n_1}^{+}\tau^{*}} + \bar{p}_{12}e^{\mathrm{i}\omega_{n_1}^{+}\tau^{*}})F_{uv_t} + p_{12}\bar{p}_{12}F_{v_tv_t}),\\
F_{1010} &= 2(F_{uu} + (p_{12} + p_{32})F_{uv} + (p_{12}e^{-\mathrm{i}\omega_{n_1}^{+}\tau^{*}} + p_{32}e^{-\mathrm{i}\omega_{n_2}^{-}\tau^{*}})F_{uv_t} + p_{12}p_{32}e^{-(\mathrm{i}\omega_{n_1}^{+}+\mathrm{i}\omega_{n_2}^{-})\tau^{*}}F_{v_tv_t}),\\
F_{1001} &= 2(F_{uu} + (p_{12} + \bar{p}_{32})F_{uv} + (p_{12}e^{-\mathrm{i}\omega_{n_1}^{+}\tau^{*}} + \bar{p}_{32}e^{\mathrm{i}\omega_{n_2}^{-}\tau^{*}})F_{uv_t} + p_{12}\bar{p}_{32}e^{(-\mathrm{i}\omega_{n_1}^{+}+\mathrm{i}\omega_{n_2}^{-})\tau^{*}}F_{v_tv_t}),\\
F_{0020} &= F_{uu} + 2p_{32}F_{uv} + 2p_{32}e^{-\mathrm{i}\omega_{n_2}^{-}\tau^{*}}F_{uv_t} + p_{32}^{2}e^{-2\mathrm{i}\omega_{n_2}^{-}\tau^{*}}F_{v_tv_t},\\
F_{0011} &= 2(F_{uu} + (p_{32} + \bar{p}_{32})F_{uv} + (p_{32}e^{-\mathrm{i}\omega_{n_2}^{-}\tau^{*}} + \bar{p}_{32}e^{\mathrm{i}\omega_{n_2}^{-}\tau^{*}})F_{uv_t} + p_{32}\bar{p}_{32}F_{v_tv_t}),\\
F_{2100} &= 3(F_{uuu} + (2p_{12} + \bar{p}_{12})F_{uuv} + (2p_{12}\bar{p}_{12} + p_{12}^{2}e^{-2\mathrm{i}\omega_{n_1}^{+}\tau^{*}})F_{uv_tv_t} + p_{12}^{2}\bar{p}_{12}e^{-\mathrm{i}\omega_{n_1}^{+}\tau^{*}}F_{v_tv_tv_t}),\\
F_{1011} &= 6(F_{uuu} + (p_{12} + p_{32} + \bar{p}_{32})F_{uuv} + (p_{32}\bar{p}_{32} + p_{12}\bar{p}_{32}e^{(-\mathrm{i}\omega_{n_1}^{+}+\mathrm{i}\omega_{n_2}^{-})\tau^{*}} + p_{12}p_{32}e^{-(\mathrm{i}\omega_{n_1}^{+}+\mathrm{i}\omega_{n_2}^{-})\tau^{*}})F_{uv_tv_t}\\
&\quad + p_{12}p_{32}\bar{p}_{32}e^{-\mathrm{i}\omega_{n_1}^{+}\tau^{*}}F_{v_tv_tv_t}),\\
F_{0021} &= 3(F_{uuu} + (2p_{32} + \bar{p}_{32})F_{uuv} + (2p_{32}\bar{p}_{32} + p_{32}^{2}e^{-2\mathrm{i}\omega_{n_2}^{-}\tau^{*}})F_{uv_tv_t} + p_{32}^{2}\bar{p}_{32}e^{-\mathrm{i}\omega_{n_2}^{-}\tau^{*}}F_{v_tv_tv_t}),\\
F_{1110} &= 6(F_{uuu} + (p_{12} + \bar{p}_{12} + p_{32})F_{uuv} + (p_{12}\bar{p}_{12} + p_{32}\bar{p}_{12}e^{(\mathrm{i}\omega_{n_1}^{+}-\mathrm{i}\omega_{n_2}^{-})\tau^{*}} + p_{12}p_{32}e^{-(\mathrm{i}\omega_{n_1}^{+}+\mathrm{i}\omega_{n_2}^{-})\tau^{*}})F_{uv_tv_t}\\
&\quad + p_{12}p_{32}\bar{p}_{12}e^{-\mathrm{i}\omega_{n_2}^{-}\tau^{*}}F_{v_tv_tv_t}),\\
F_{0200} &= \overline{F_{2000}},\quad F_{0110} = \overline{F_{1001}},\quad F_{0101} = \overline{F_{1010}},\quad F_{0002} = \overline{F_{0020}}.
\end{aligned}
$$

Denote $f_{q_1q_2q_3q_4}^{1(k)} = \sqrt{\frac{1}{l\pi}}\psi_k(0)F_{q_1q_2q_3q_4}, (q_1+q_2+q_3+q_4=2)$.